IEEE Access
Multidisciplinary | Rapid Review | Open Access Journal

Received August 8, 2019, accepted August 27, 2019, date of publication September 9, 2019, date of current version September 23, 2019.

Digital Object Identifier 10.1109/ACCESS.2019.2940027

Joint Tracking and Classification of Extended Targets Using Random Matrix and Bernoulli Filter for Time-Varying Scenarios

LIPING WANG[1], YUAN HUANG[2], RONGHUI ZHAN[1], AND JUN ZHANG[1]
[1]Science and Technology on Automatic Target Recognition Laboratory, National University of Defense Technology, Changsha 410073, China
[2]Space Information Processing Center, National University of Defense Technology, Changsha 410073, China

Corresponding author: Ronghui Zhan (zhanrh@nudt.edu.cn)

This work was supported by the National Natural Science Foundation of China under Grant 61471370.

ABSTRACT In surveillance applications, the extent states and measurements of extended targets received by sensors are time-varying. In this paper, we propose a joint tracking and classification (JTC) method for single extended target under the presence of clutter and detection uncertainty. The extent state is modeled as elliptic shape via random matrix model (RMM), and is used as the feature for target classification. To adapt to the time-varying conditions of an extended target, the RMM proposed by Lan et al. is used. Besides, the RMM is integrated into Bernoulli filter to detect an extended target with clutter and detection uncertainty. The resulting method is called joint tracking and classification Gaussian inverse Wishart Bernoulli (JTC-GIW-Ber) filter, and the closed expressions for JTC-GIW-Ber filter recursions are derived under the necessary assumptions and approximations. Comprehensive simulations are carried out to test the performance, and the results demonstrate that the proposed JTC-GIW-Ber filter not only outperforms the JTC-GIW probability hypothesis density (JTC-GIW-PHD) filter and the GIW-Ber filter in extent state estimation, but also outperforms the JTC-GIW-PHD filter in target classification.

INDEX TERMS Bernoulli filter, joint tracking and classification, random matrix model, single extended target.

I. INTRODUCTION

In many civil and military applications such as surveillance, target tracking and target classification are two critical problems. Target tracking is a problem about estimating the target state, and target classification is a problem about determining the target class. These two problems are usually interdependent. For example, target tracking could affect target classification by providing kinematic and size information of different classes, and target classification could affect target tracking via using class-dependent motion models. Therefore, it is necessary to simultaneously deal with target tracking and classification under a unified interactive framework, that is, joint tracking and classification(JTC). JTC methods provide an effective way to overcome the shortcomings of isolated processing in traditional target tracking and target classification [1]–[7].

The associate editor coordinating the review of this manuscript and approving it for publication was Yue Zhang.

For the early low resolution sensors, at most one measurement will be generated for a single target. Accordingly, the targets are called point targets. Considering the different way of measurement information utilization, the JTC methods for point targets can be roughly divided into two categories: 1) kinematic information based methods [4], [5], and 2) attribute information based methods [6], [7]. For kinematic information based JTC methods, the motion property of targets (including velocity and acceleration ability) can be used for classification. For example, by using the acceleration ability limits, static class-matched filters are designed for aircraft targets JTC in [4]. By using velocity constraints, both the class-dependent velocity likelihoods and the kinematic measurement likelihoods are used to improve the accuracy of classification in, [5]. For attribute information based JTC methods, extra sensor is required to obtain the target attribute, typical application examples can be found in, [6] and [7], where electronic support measures (ESM) are used to provide attribute measurement data.

Due to rapid advances in sensor technology in recent years, it becomes increasingly common that targets occupy several sensor resolution cells and generate at least one measurement at each time step. Therefore, the targets are called extended targets [8]. The more sufficient information obtained by high resolution sensors can facilitate extended target classification. However, in the real application environment, the classification feature originated from extended target is probably time-varying, and needs to be modeled as extent state in the estimate process. Therefore, for extended targets JTC, not only kinematic state but also extent state needs to be estimated. The extent state describes the spatial expansion of the extended targets, and it mainly contains information such as shapes (ellipse, rectangle, or other complex arbitrary shapes), size, and orientation. The extent state can be estimated by the random matrix model (RMM) [9]–[11], the random hypersurface model (RHM) [12]–[14], the Gaussian processes model [15], [16], and so on. Compared with the JTC methods of point targets, the extent state can be used as the feature for target classification. For example, Lan and Li [1] proposed JTC method of extended targets using RMM and the prior information of target size. Based on the support function, Sun *et al.* [17] proposed the JTC method of extended targets using RMM. Magnant *et al.* [18] took advantage of target extent measurements and proposed a JTC algorithm for extended targets. However, these previous methods did not address the issues of tracking multiple extended targets with unknown number, or with clutter and detection uncertainty. To solve these problems, Hu *et al.* [19] proposed a JTC method for maneuvering extended multi-target based on probability hypothesis density (PHD) filter [20] and RMM. Nevertheless, the PHD filter is the first moment approximation of multi-objective Bayesian filters, and performs relatively poor in cardinality estimation. Besides, extra multi-target extraction is needed for the PHD filter [21]. The Bernoulli filter is an exact Bayesian single-target detector/tracker [22], and it was used to address the point targets JTC problem in [23] and [24]. As for extended target JTC, no much work has been found in the framework of Bernoulli filter currently.

For JTC methods of point targets, the effectiveness of kinematic information based JTC methods will be greatly reduced when targets have similar speed or acceleration, and the attribute information based JTC methods have to rely on extra measurements information. In contrast, the JTC methods of extended targets based on the extent state have better robustness and need no extra sensor measurement information. For sea surveillance, the ship shape can be well represented by an elliptical shape, and the successful application examples of extended target tracking using X-Band radar data are presented in [25]–[27]. In this paper, we propose a joint tracking and classification Gaussian inverse Wishart Bernoulli (JTC-GIW-Ber) filter by using the extent state as the feature for classification. In the proposed method, we adopt the random matrix to model the extended target as ellipse for the reason that RMM has a concise closed expression, and we only use simulated data to perform experiments in view of the unavailability of real radar data.

In summary, the main contributions of this paper are as follows: 1) the JTC-GIW-Ber filter is proposed for single extended target under the presence of clutter and detection uncertainty. 2) closed expressions for the proposed JTC-GIW-Ber filter recursions are derived. 3) the proposed JTC-GIW-Ber filter is compared with the GIW-Ber filter and the JTC-GIW-PHD filter under the time-varying scenarios.

The rest of this paper is organized as follows. Section II starts with a brief review of the problem formulation and Bernoulli filter for the extended target. Then the proposed JTC-GIW-Ber filter and its closed expression are described in Section III. Simulation results are presented in Section IV. Finally, conclusions are given in Section V.

For the sake of clarity and readability, the symbolic representation of variables in this paper obeys the following rules. Minor non-bold letters, e.g., k, j, represent scalars. Minor bold letters, e.g., $\boldsymbol{x}, \boldsymbol{z}$, represent vectors. Capital non-bold letters, e.g., X, Z, represent matrices. Capital bold letters, e.g., $\boldsymbol{X}, \boldsymbol{Z}$, represent sets. Some notations and distributions used in this paper are summarized in Table 1.

II. BACKGROUND

A. PROBLEM FORMULATION

For extended targets, the target state consists of the kinematic state and the extent state. In this paper, $\boldsymbol{x}_k = (\boldsymbol{r}_k^{\mathrm{T}}, \dot{\boldsymbol{r}}_k^{\mathrm{T}}, \ddot{\boldsymbol{r}}_k^{\mathrm{T}})^{\mathrm{T}}$ represents kinematic state, where the vectors $\boldsymbol{r}_k$, $\dot{\boldsymbol{r}}_k$, and $\ddot{\boldsymbol{r}}_k$ are the spatial position, velocity and acceleration, respectively, with the dimension of target motion space d. In this paper, we assume that the target moves in a two-dimensional space, which means that $d = 2$. The dimension of the kinematic state vector $\boldsymbol{x}_k$ is $3d \times 1$. In the framework of RMM, the extent state is modeled by a symmetric positive define (SPD) random matrix X_k with the dimension of $d \times d$. In order to express more concisely, $\xi_k \triangleq (\boldsymbol{x}_k, X_k)$ is used to represent the state of an extended target. For the convenience of subsequent formula derivation, the operation sign $\otimes$ is used to define the Kronecker product of two matrices.

The kinematic state dynamics is modeled as:

$$\boldsymbol{x}_k = (F_{k|k-1} \otimes I_d)\boldsymbol{x}_{k-1} + \boldsymbol{v}_k, \tag{1}$$

where, $F_{k|k-1} \otimes I_d$ is the state transition function, I_d is a $d \times d$ identity matrix, and $\boldsymbol{v}_k$ is the process noise following Gaussian distribution, i.e., $\mathcal{N}(\boldsymbol{v}_k; 0, Q_{k|k-1} \otimes X_k)$. This distribution of the process noise indicates that the kinematic state $\boldsymbol{x}_k$ is affected by the extent state X_k. $F_{k|k-1}$ and $Q_{k|k-1}$ are given by:

$$F_{k|k-1} = \begin{bmatrix} 1 & t_{\mathrm{s}} & \frac{t_{\mathrm{s}}^2}{2} \\ 0 & 1 & t_{\mathrm{s}} \\ 0 & 0 & e^{-\frac{t_{\mathrm{s}}}{\theta}} \end{bmatrix}, \tag{2}$$

$$Q_{k|k-1} = \Sigma^2(1 - e^{-2t_{\mathrm{s}}/\theta})\mathrm{diag}\left([\,0 \quad 0 \quad 1\,]\right), \tag{3}$$

where, Σ is the scalar acceleration value and t_{s} is the sampling time. θ is the maneuver correlation time constant. The diag$(\cdot)$

TABLE 1. List of mathematical symbols and probability distributions.

$\boldsymbol{x}_k$	Kinematic state of a target at time k
X_k	Extent state of a target at time k
$\boldsymbol{X}_k$	Random finite set (RFS) of target state at time k
$\boldsymbol{z}_k$	Single measurement vector at time k
$\boldsymbol{Z}_k$	Measurement RFS at time k
$\boldsymbol{Z}^k$	Measurement RFS from time 1 up to time k
q_k	Posterior probability of target existence at time k
$\mathcal{S}_k$	Posterior spatial probability density function (PDF) of Bernoulli filter at time k
$\lvert\boldsymbol{W}\rvert$	Cardinality of set $\boldsymbol{W}$, i.e., number of elements in set $\boldsymbol{W}$
$\lvert V\rvert$	Determinant of matrix V
$\mathrm{etr}(A)$	The abbreviation of exponential trace $\exp[\mathrm{tr}(A)]$
$\mathbb{R}^n$	A real n dimensional vector space
$\mathbb{S}_+^n$	A $n \times n$ random positive semi-define matrix space
$\mathbb{S}_{++}^n$	A $n \times n$ random symmetric positive define (SPD) matrix space
$\mathcal{N}(\boldsymbol{x}; \boldsymbol{m}, P)$	Gaussian distribution defined over the variable $\boldsymbol{x} \in \mathbb{R}^n$ with mean vector $\boldsymbol{m} \in \mathbb{R}^n$ and covariance matrix $P \in \mathbb{S}_+^n$. The PDF is given by $(2\pi)^{-n/2}\lvert P\rvert^{-1/2}\mathrm{etr}\left(-P^{-1}(\boldsymbol{x}-\boldsymbol{m})(\boldsymbol{x}-\boldsymbol{m})^{\mathrm{T}}/2\right)$. n denotes the space dimension of vector $\boldsymbol{x}$.
$\mathcal{IW}(X; v, V)$	Inverse Wishart distribution defined over the matrix $X \in \mathbb{S}_{++}^n$ with freedom degree $v > 2n$ and inverse matrix $V \in \mathbb{S}_{++}^n$. The PDF is given by $2^{-\frac{(v-n-1)n}{2}}\lvert V\rvert^{\frac{v-n-1}{2}}\left(\Gamma_n(\frac{v-n-1}{2})\lvert X\rvert^{\frac{v}{2}}\right)^{-1}$ $\mathrm{etr}(-\frac{X^{-1}V}{2})$. $\Gamma_n(\cdot)$ is the multi-variable gamma function with dimension n.
$\mathcal{W}(X; c, \psi)$	Wishart distribution defined over the matrix $X \in \mathbb{S}_{++}^n$ with freedom degree $c \geq n$ and inverse matrix $\psi \in \mathbb{S}_{++}^n$. The PDF is given by $\left(2^{\frac{cn}{2}}\Gamma_n(\frac{c}{2})\lvert\psi\rvert^{\frac{c}{2}}\right)^{-1}\lvert X\rvert^{\frac{c-n-1}{2}}\mathrm{etr}(-\frac{\psi^{-1}X}{2})$.
$\mathcal{PS}(\lvert\boldsymbol{W}\rvert; \lambda)$	The Poisson distribution with average rate $\lambda \in \mathbb{R}^+$ and a scalar variable $\lvert\boldsymbol{W}\rvert \in \mathbb{R}^+$. The PDF is given by $\frac{e^{-\lambda}\lambda^{\lvert\boldsymbol{W}\rvert}}{\lvert\boldsymbol{W}\rvert!}$.
$\mathcal{BI}(\lvert\boldsymbol{W}\rvert; l, p)$	The Binomial distribution with number of binary experiments $l \in \mathbb{R}^+$ and the probability of success of each of the experiments $\mathcal{P} \in [0, 1]$. The PDF is given by $\frac{l!}{(l-\lvert\boldsymbol{W}\rvert)!}\mathcal{P}^{\lvert\boldsymbol{W}\rvert}(1-\mathcal{P})^{l-\lvert\boldsymbol{W}\rvert}$.

denotes a diagonal matrix with the elements of vector on the main diagonal.

$\boldsymbol{Z}_k = \{\boldsymbol{z}_k^m\}_{m=1}^{n_k}$ is a set with n_k position measurements received at time k. The measurement model for an extended target is given by:

$$\boldsymbol{z}_k^m = H_k\boldsymbol{x}_k + \boldsymbol{e}_k^m, \quad m = 1, \cdots, n_k, \tag{4}$$

where, $H_k = (\boldsymbol{h}_k \otimes I_d)$, $\boldsymbol{h}_k = [1\ 0\ 0]$, and $\boldsymbol{e}_k^m$ is Gaussian white noise.

According to the Bayesian theory and RMM, the estimator can obtain the probability density function (PDF) $p(\boldsymbol{x}_k, X_k|\boldsymbol{Z}^k)$ based on the measurement set $\boldsymbol{Z}_k$ at time k and the PDF $p(\boldsymbol{x}_{k-1}, X_{k-1}|\boldsymbol{Z}^{k-1})$ at time $k-1$. The kinematic state is modeled by the Gaussian distribution, that is, $\mathcal{N}(\boldsymbol{x}_k; \boldsymbol{m}_k, P_k \otimes X_k)$. The $P_k \otimes X_k$ indicates that the estimated kinematic state $\boldsymbol{x}_k$ is affected by the extent state X_k. The extent state is modeled by the inverse Wishart distribution, that is, $\mathcal{IW}(X_k; v_k, V_k)$. Under the assumption $p(\boldsymbol{x}_{k-1}, X_{k-1}|\boldsymbol{Z}^{k-1}) = \mathcal{N}(\boldsymbol{x}_{k-1}; \boldsymbol{m}_{k-1}, P_{k-1} \otimes X_{k-1})\mathcal{IW}(X_{k-1}; v_{k-1}, V_{k-1})$, $p(\boldsymbol{x}_k, X_k|\boldsymbol{Z}^k)$ turns out to be $\mathcal{N}(\boldsymbol{x}_k; \boldsymbol{m}_k, P_k \otimes X_k)\mathcal{IW}(X_k; v_k, V_k)$ by two-step operation of prediction and update. More complex dynamical variation of extent state and practical observation distortion are considered in [11], and we use the same RMM in this paper. Therefore, the evolution model of extent state is given by

$$p(X_k|X_{k-1}) = \mathcal{W}(X_k; \delta_k, A_kX_{k-1}A_k^{\mathrm{T}}), \tag{5}$$

where, δ_k is the freedom parameter, and A_k is a $d \times d$ matrix which shows the specific dynamic evolution mode of the extent state.

For the measurement noise $\boldsymbol{e}_k^m$, it is modeled by

$$\mathcal{N}(\boldsymbol{e}_k^m; 0, B_kX_kB_k^{\mathrm{T}}), \tag{6}$$

where B_k is a $d \times d$ matrix which describes the distortion of the extent state in terms of size, shape and orientation.

B. BERNOULLI FILTER FOR AN EXTENDED TARGET

A random finite set (RFS) is a set with finite elements [28], [29]. The number of elements in the set is random and each element is a random variable. Besides, the elements in the set are unordered. Three random finite sets (RFSs) are used in the Bernoulli filter for an extended target: Bernoulli RFS, Poisson RFS, and Binomial RFS. Poisson RFS and Binomial RFS are special cases of the independent identically distributed (i.i.d) cluster RFS. For the Bernoulli filter of an extended target, target state at time k is modeled by the Bernoulli RFS. The sensor measurements are composed of target measurements and clutter measurements, both of which are defined as RFSs. Measurements originating from the extended target are defined as Binomial RFS. The clutter measurements are modeled by Poisson RFS.

1) BERNOULLI RFS

Bernoulli RFS can either be an empty set $\varnothing$ with probability $1-q$ or be a single element set with probability q and PDF $\mathcal{S}(\xi)$. The finite set statistics (FISST) PDF of a Bernoulli RFS $\boldsymbol{X}$ is

$$f(\boldsymbol{X}) = \begin{cases} 1-q & \text{if } \boldsymbol{X} = \emptyset, \\ q\mathcal{S}(\xi) & \text{if } \boldsymbol{X} = \{\xi\}. \end{cases} \tag{7}$$

2) i.i.d CLUSTER RFS

The elements of i.i.d cluster RFS $\boldsymbol{X}$ are independently and identically distributed. The spatial distribution function(i.e. PDF) of these elements is $\mathcal{S}(\xi)$ and the distribution of cardinality $|\boldsymbol{X}|$ is $\rho(|\boldsymbol{X}|)$. The FISST PDF of a i.i.d cluster RFS $\boldsymbol{X}$ is

$$f(\boldsymbol{X}) = |\boldsymbol{X}|!\rho(|\boldsymbol{X}|)\prod_{\xi\in\boldsymbol{X}}\mathcal{S}(\xi). \tag{8}$$

3) POISSON RFS

When the cardinality distribution $\rho(|\boldsymbol{X}|)$ in the i.i.d cluster RFS obeys Poisson distribution, the i.i.d cluster RFS becomes Poisson RFS with the FISST PDF

$$f(\boldsymbol{X}) = e^{-\lambda}\prod_{\xi\in\boldsymbol{X}}\lambda\mathcal{S}(\xi), \tag{9}$$

where λ is the Poisson average rate.

4) BINOMIAL RFS

When the cardinality distribution $\rho(|\boldsymbol{X}|)$ in the i.i.d cluster RFS obeys Binomial distribution, the i.i.d cluster RFS becomes Binomial RFS with the FISST PDF

$$f(\boldsymbol{X}) = \frac{l!}{(l-|\boldsymbol{X}|)!}\mathcal{P}^{|\boldsymbol{X}|}(1-\mathcal{P}^{|\boldsymbol{X}|})^{l-|\boldsymbol{X}|}\prod_{\xi\in\boldsymbol{X}}\mathcal{S}(\xi), \quad (10)$$

where l is the number of binary experiments and $\mathcal{P}$ is the probability of experiment success.

For target tracking, the Bernoulli filter [22] propagates the posterior probability of target existence $q_k = P(|\boldsymbol{X}| = 1|\boldsymbol{Z}^k)$ and the posterior spatial PDF $\mathcal{S}_k(\xi) = p(\xi|\boldsymbol{Z}^k)$. The prediction equations of Bernoulli filters are:

$$q_{k|k-1} = p_{\mathrm{B}}(1-q_{k-1}) + p_{\mathrm{S}}q_{k-1}, \quad (11)$$

$$\mathcal{S}_{k|k-1}(\xi) = \frac{p_{\mathrm{B}}(1-q_{k-1})\mathcal{S}_{k|k-1,\mathrm{B}}(\xi)}{q_{k|k-1}} + \frac{p_{\mathrm{S}}q_{k-1}\int\pi_{k|k-1}(\xi|\xi')\mathcal{S}_{k-1}(\xi')d\xi'}{q_{k|k-1}}, \quad (12)$$

where, p_{B} and p_{S} are the probability of target birth and target survival, respectively. $\pi_{k|k-1}(\xi|\xi')$ is the transitional density which describes the target state evolving from ξ' to ξ. The PDF $\mathcal{S}_{k|k-1,\mathrm{B}}(\xi)$ denotes the PDF of birth targets.

It is assumed that at time k, the target consists of l_k measurements (target originated measurement points) with the probability of detection p_{D}, and the spatial distribution of clutter is $\mathcal{C}(\boldsymbol{z})$ with Poisson average rate λ. Due to the uncertainty of detection, an extended target can produce zero, one or more detection. Therefore, when multiple measurements are received, all the possibilities of measurement partition need to be traversed, that is, $\boldsymbol{W} \in \boldsymbol{P}_{1:l_k}(\boldsymbol{Z}_k)$, where $\boldsymbol{P}_{1:l_k}(\boldsymbol{Z}_k)$ is the set of all subsets of $\boldsymbol{Z}_k$ with cardinalities equal to $1, 2, \cdots, l_k$. The Bernoulli filter update equations are:

$$q_k = \frac{1-\Delta_k}{1-q_{k|k-1}\Delta_k}q_{k|k-1}, \quad (13)$$

$$\mathcal{S}_k(\xi) = \frac{(1-p_{\mathrm{D}})^{l_k} + \sum_{\boldsymbol{W}\in\boldsymbol{P}_{1:l_k}(\boldsymbol{Z}_k)}\psi_k\prod_{z\in\boldsymbol{W}}\frac{g_k(z|\xi)}{\lambda\mathcal{C}(z)}}{1-\Delta_k}\mathcal{S}_{k|k-1}(\xi), \quad (14)$$

$$\Delta_k = 1-(1-p_{\mathrm{D}})^{l_k} - \sum_{\boldsymbol{W}\in\boldsymbol{P}_{1:l_k}(\boldsymbol{Z}_k)}\psi_k\frac{\int\prod_{z\in\boldsymbol{W}}g_k(z|\xi)\mathcal{S}_{k|k-1}(\xi)d\xi}{\prod_{z\in\boldsymbol{W}}\lambda\mathcal{C}(z)}, \quad (15)$$

$$\psi_k = \frac{l_k!}{(l_k-|\boldsymbol{W}|)!}\frac{p_{\mathrm{D}}^{|\boldsymbol{W}|}}{(1-p_{\mathrm{D}})^{|\boldsymbol{W}|-l_k}}, \quad (16)$$

where $g_k(z|\xi)$ is the likelihood function. Due to the fact that l_k is unknown, we need to calculate the l_k using the received measurements. First, the cluster processing using the distance partitioning will generate $n_{\boldsymbol{W}}$ subsets $\boldsymbol{W}^{(m)}$, $m = 1, \cdots, n_{\boldsymbol{W}}$. Then the value of l_k can be obtained by:

$$\boldsymbol{W}_{\max} = \max\left\{\left|\boldsymbol{W}^{(1)}\right|, \left|\boldsymbol{W}^{(2)}\right|, \cdots, \left|\boldsymbol{W}^{(n_{\boldsymbol{W}})}\right|\right\}, \quad (17)$$

$$l_k = \mathrm{round}\left(\frac{\boldsymbol{W}_{\max}}{p_{\mathrm{D}}}\right). \quad (18)$$

where round$(\cdot)$ denotes rounding towards the nearest integer.

The GIW-Ber filter presented in [30] integrates the RMM [9] into the Bernoulli filter. However, the measurement noise and the more complex dynamical variation are not taken into consideration in the method proposed in [9], and these two problems are solved by the RMM proposed in [11]. Therefore, we use the RMM in [11] to improve the GIW-Ber filter in [30], and the improved GIW-Ber is used as a class-dependent filter for the proposed JTC-GIW-Ber filter in this paper.

III. JTC ALGORITHM BASED ON BERNOULLI FILTER AND RANDOM MATRIX FRAMEWORK

A. THE PROPOSED JTC-GIW-BER FILTER

For JTC, $(\boldsymbol{x}_k, X_k, \boldsymbol{c})$ is used to remodel an extended target at time k, where $\boldsymbol{c}= (c^1, c^2, \cdots, c^{n_c})$. n_c indicates the number of known possible target classes, and c^i represents the ith target class. From the point of Bayesian filter, the JTC is in essence used to obtain the probability density-mass function (PDMF) of the extended target

$$p(\boldsymbol{x}_k, X_k, \boldsymbol{c}|\boldsymbol{Z}^k) = p(\boldsymbol{x}_k, X_k|\boldsymbol{c}, \boldsymbol{Z}^k)p(\boldsymbol{c}|\boldsymbol{Z}^k) = \sum_{i=1}^{n_c}p(\boldsymbol{x}_k, X_k|c^i, \boldsymbol{Z}^k)p(c^i|\boldsymbol{Z}^k), \quad (19)$$

where $p(\boldsymbol{x}_k, X_k|c^i, \boldsymbol{Z}^k)$ and $p(c^i|\boldsymbol{Z}^k)$ represent target state estimation and probability of target class, respectively.

For target tracking, using the Bayesian formulas, the PDF of $p(\boldsymbol{x}_k, X_k|c^i, \boldsymbol{Z}^k)$ can be obtained under the one-order Markov state transition assumption, i.e.,

$$p(\boldsymbol{x}_k, X_k|c^i, \boldsymbol{Z}^k) = \frac{p(\boldsymbol{Z}_k|\boldsymbol{x}_k, X_k, c^i, \boldsymbol{Z}^{k-1})p(\boldsymbol{x}_k, X_k|c^i, \boldsymbol{Z}^{k-1})}{p(\boldsymbol{Z}_k|c^i, \boldsymbol{Z}^{k-1})}. \quad (20)$$

In (20), the $p(\boldsymbol{Z}_k|c^i, \boldsymbol{Z}^{k-1}) = \int p(\boldsymbol{Z}_k|\boldsymbol{x}_k, X_k, c^i, \boldsymbol{Z}^{k-1})p(\boldsymbol{x}_k, X_k|c^i, \boldsymbol{Z}^{k-1})d\boldsymbol{x}_k dX_k$ is the normalized parameter. For simplification, $\Lambda_k^i \triangleq p(\boldsymbol{Z}_k|c^i, \boldsymbol{Z}^{k-1})$. Therefore, (20) becomes

$$p(\boldsymbol{x}_k, X_k|c^i, \boldsymbol{Z}^k) = (\Lambda_k^i)^{-1}p(\boldsymbol{Z}_k|\boldsymbol{x}_k, X_k, c^i, \boldsymbol{Z}^{k-1})p(\boldsymbol{x}_k, X_k|c^i, \boldsymbol{Z}^{k-1}), \quad (21)$$

For target classification, using the total probability principle and Bayesian formulas, the probability mass function (PMF) of $\mu_k^i \triangleq p(c^i|\boldsymbol{Z}^k)$ can be obtained as

$$\mu_k^i = \frac{p(\boldsymbol{Z}_k|c^i, \boldsymbol{Z}^{k-1})p(c^i|\boldsymbol{Z}^{k-1})}{p(\boldsymbol{Z}_k|\boldsymbol{Z}^{k-1})}, \quad (22)$$

where $p(\boldsymbol{Z}_k|\boldsymbol{Z}^{k-1}) = \sum_{i=1}^{n_c}p(\boldsymbol{Z}_k|c^i, \boldsymbol{Z}^{k-1})p(c^i|\boldsymbol{Z}^{k-1})$ is the normalized parameter and can be defined as ∇_k. Therefore, we have $\nabla_k = \sum_{i=1}^{n_c}\Lambda_k^i\mu_{k-1}^i$ and (22) can be rewritten in a

more compact form as:

$$\begin{aligned}\mu_k^i &= (\nabla_k)^{-1} p(\boldsymbol{Z}_k|c^i, \boldsymbol{Z}^{k-1}) p(c^i \mid \boldsymbol{Z}^{k-1}) \\ &= (\nabla_k)^{-1} \Lambda_k^i \mu_{k-1}^i. \end{aligned} \tag{23}$$

For extended targets, the extent state may contain the size, shape, and orientation information. In the RMM, the extent state is modeled as elliptic shape using a SPD matrix X_k. For elliptic targets, their sizes are determined by major and minor axes. Therefore, the concrete expression of extent state is $X_k = M_k \text{diag}([(a_k/2)^2, (b_k/2)^2]) M_k^{\text{T}}$, where M_k is the rotation matrix which is determined by the orientation angle. a_k and b_k are the lengths of major and minor axes at time k, respectively. For JTC of extended targets, the extent state can be used as the feature for target classification. Because the target is moving, and orientation angle of the extended state changes as the target moves. However, the shape and size of extent state are known as a priori information for a specific target class. In this paper, we use SPD matrix to model class-dependent shape and size information, and the corresponding extent state is called the class-dependent extent state, that is, $Z^{p,i} \in \mathbb{S}_{++}^n$. The $Z^{p,i}$ is a variable, and its value is related to the target class i. In case of no rotation (the major axis of the ellipse is parallel to X axis), the mathematical expression of the class-dependent extent state is $Z^{p,i} = \text{diag}([(a_i/2)^2, (b_i/2)^2])$. a_i and b_i are the lengths of major and minor axes of the target class i, respectively. The class-dependent extent state can be regarded as the pseudo-measurement information, which is not directly obtained by senors, but can be used as the prior information for JTC.

Based on the above analysis, the extent state X_k and pseudo-measurements $Z^{p,i}$ have the following relationship

$$X_k = (E_k^i)^{-1} Z^{p,i} (E_k^i)^{-\text{T}}, \tag{24}$$

where the $(E_k^i)^{-1}$ is rotation matrix. In this paper, we assume that the orientation angle of a target is same as the velocity direction. Therefore, the rotation matrix $(E_k^i)^{-1}$ is

$$(E_k^i)^{-1} = \begin{bmatrix} \cos(\theta_k) & -\sin(\theta_k) \\ \sin(\theta_k) & \cos(\theta_k) \end{bmatrix}, \quad \theta_k = \arctan\left(\frac{\boldsymbol{x}_k(4)}{\boldsymbol{x}_k(3)}\right). \tag{25}$$

The transitional density of extent state is modeled as Wishart distribution. Similarly, the transitional density of the pseudo-measurements $Z^{p,i}$ from target class i and the extent state X_k can be modeled as:

$$p(Z^{p,i}|c^i, X_k) = \mathcal{W}(Z^{p,i}; \delta_k^{p,i}, E_k^i X_k (E_k^i)^{\text{T}} / \delta_k^{p,i}). \tag{26}$$

where $\delta_k^{p,i}$ is the freedom parameter.

Since the pseudo-measurements $\{Z^{p,i}\}_{i=1}^{n_c}$ can be obtained as a priori information at each time, the available measurements $\boldsymbol{\mathcal{Z}}_k$ at time k include both real measurements and pseudo-measurements:

$$\boldsymbol{\mathcal{Z}}_k = \left\{ \boldsymbol{Z}_k, \{Z^{p,i}\}_{i=1}^{n_c} \right\}. \tag{27}$$

Therefore, (19), i.e., PDMF for JTC of an extended target becomes

$$\begin{aligned} p(\boldsymbol{x}_k, X_k, \boldsymbol{c}|\boldsymbol{\mathcal{Z}}^k) &= p(\boldsymbol{x}_k, X_k|\boldsymbol{c}, \boldsymbol{\mathcal{Z}}^k) p(\boldsymbol{c}|\boldsymbol{\mathcal{Z}}^k) \\ &= \sum_{i=1}^{n_c} p(\boldsymbol{x}_k, X_k|c^i, \boldsymbol{\mathcal{Z}}^k) p(c^i|\boldsymbol{\mathcal{Z}}^k). \end{aligned} \tag{28}$$

Equation (21) for target tracking becomes

$$\begin{aligned} p(\boldsymbol{x}_k, X_k|c^i, \boldsymbol{\mathcal{Z}}^k) = (\tilde{\Lambda}_k^i)^{-1} p(\boldsymbol{\mathcal{Z}}_k|\boldsymbol{x}_k, X_k, c^i, \boldsymbol{\mathcal{Z}}^{k-1}) \\ \times p(\boldsymbol{x}_k, X_k|c^i, \boldsymbol{\mathcal{Z}}^{k-1}), \end{aligned} \tag{29}$$

where $\tilde{\Lambda}_k^i = \int p(\boldsymbol{\mathcal{Z}}_k|\boldsymbol{x}_k, X_k, c^i, \boldsymbol{\mathcal{Z}}^{k-1}) p(\boldsymbol{x}_k, X_k|c^i, \boldsymbol{\mathcal{Z}}^{k-1}) d\boldsymbol{x}_k dX_k$.

Equation (23) for target classification becomes

$$\begin{aligned} \tilde{\mu}_k^i &= (\tilde{\nabla}_k)^{-1} p(\boldsymbol{\mathcal{Z}}_k|c^i, \boldsymbol{\mathcal{Z}}^{k-1}) p(c^i|\boldsymbol{\mathcal{Z}}^{k-1}) \\ &= (\tilde{\nabla}_k)^{-1} \tilde{\Lambda}_k^i \tilde{\mu}_{k-1}^i, \end{aligned} \tag{30}$$

where, $\tilde{\mu}_k^i \triangleq p(c^i|\boldsymbol{\mathcal{Z}}^k)$ and $\tilde{\nabla}_k \triangleq p(\boldsymbol{\mathcal{Z}}_k|\boldsymbol{\mathcal{Z}}^{k-1}) = \sum_{i=1}^{n_c} \tilde{\Lambda}_k^i \tilde{\mu}_{k-1}^i$.

For tracking, the number and state of targets may vary with time due to the existence of target birth and death situations. In this paper, we propose joint tracking and classification filter for single extended target based on RMM and Bernoulli filter (JTC-GIW-Ber filter) for the time-varying scenario. In this time-varying scenario, the number of detected measurements and extent state of an extended target are varying along with the target range. The proposed JTC-GIW-Ber filter uses the extent state as the feature information for classification. Compared with kinematic information based JTC methods and attribute information based JTC methods, the proposed JTC-GIW-Ber filter does not have to depend on target maneuver or additional senor's attribute information, and it only needs the position measurement information generated by high resolution sensors to achieve JTC. Besides, the proposed JTC-GIW-Ber filter can deal with the presence of the detection uncertainty and clutter.

An extended target at time $k-1$ is modeled as $\boldsymbol{X}_{k-1} = \varnothing$ or $\boldsymbol{X}_{k-1} = \left\{ \sum_{i=1}^{n_c} \xi_{k-1}^i \tilde{\mu}_{k-1}^i \right\}$, where n_c is the number of target classes. ξ_{k-1}^i and $\tilde{\mu}_{k-1}^i$ are the state and the class probability of the ith target class at time $k-1$. The closed expressions for the proposed JTC-GIW-Ber filter recursions are derived under the following assumptions.

Assumption 1: The kinematic part of a target follows a linear Gaussian dynamical model, the sensor has a linear Gaussian measurement model.

Assumption 2: The clutter is modeled as Poisson RFS, and it is independent of target-originated measurements. The PDF of clutter is a uniform distribution.

Assumption 3: The measurements of extended targets are modeled as Binomial RFS.

Assumption 4: The survival and detection probabilities are state independent, i.e., $p_{\text{S}}(\xi_k) = p_{\text{S}}$ and $p_{\text{D}}(\xi_k) = p_{\text{D}}$.

Based on the Assumptions 1–4, the proposed JTC-GIW-Ber filter also includes two steps: prediction and update.

In this paper, the superscript i denotes the target class, superscript (j) denotes the jth GIW component, and superscript $(j, \boldsymbol{W})$ denotes the jth updated GIW component using the $\boldsymbol{W}$ measurement set.

1) PREDICTION STEP

Under linear Gaussian assumption as (1), it is possible to propagate the spatial PDF $\mathcal{S}_{k-1}(\xi)$ as a GIW mixture at time $k-1$, i.e.,

$$\mathcal{S}_{k-1}(\xi) = \sum_{j=1}^{\mathcal{J}_{k-1}} \sum_{i=1}^{n_c} w_{k-1}^{(j),i} \mathcal{N}(\boldsymbol{x}; \boldsymbol{m}_{k-1}^{(j),i}, P_{k-1}^{(j),i} \otimes X) \times \mathcal{IW}(X; v_{k-1}^{(j),i}, V_{k-1}^{(j),i}) \tilde{\mu}_{k-1}^{(j),i}, \quad (31)$$

where, $\mathcal{J}_{k-1}$ and n_c are the number of GIW components and target classes at time $k-1$, respectively. $w_{k-1}^{(j),i}$ is the weight of the jth GIW component of target class i at time $k-1$. $\tilde{\mu}_{k-1}^{(j),i}$ is the probability of the jth GIW component of target class i.

In this paper, the PDF of birth targets is also considered as a mixture of GIW at time k, i.e.,

$$\mathcal{S}_{k,\mathrm{B}}(\xi) = \sum_{j=1}^{\beta_k} \sum_{i=1}^{n_\mathrm{B}} w_{k,\mathrm{B}}^{(j),i} \mathcal{N}\left(\boldsymbol{x}; \boldsymbol{m}_{k-1,\mathrm{B}}^{(j),i}, P_{k-1,\mathrm{B}}^{(j),i} \otimes X\right) \times \mathcal{IW}\left(X; v_{k-1,\mathrm{B}}^{(j),i}, V_{k-1,\mathrm{B}}^{(j),i}\right) \tilde{\mu}_{k,\mathrm{B}}^{(j),i}, \quad (32)$$

where, β_k and n_B are the number of GIW components and target classes of birth targets, respectively. $w_{k,\mathrm{B}}^{(j),i}$ is the weight of the jth GIW component for target class i. $\tilde{\mu}_{k,\mathrm{B}}^{(j),i} = 1/n_\mathrm{B}$ is the class probability of new birth targets.

Then, the predicted state is also GIW mixture,

$$\mathcal{S}_{k|k-1}(\xi) = \sum_{j=1}^{\mathcal{J}_{k|k-1}} \sum_{i=1}^{n_c} w_{k|k-1}^{(j),i} \mathcal{N}\left(\boldsymbol{x}; \boldsymbol{m}_{k|k-1}^{(j),i}, P_{k|k-1}^{(j),i} \otimes X\right) \times \mathcal{IW}\left(X; v_{k|k-1}^{(j),i}, V_{k|k-1}^{(j),i}\right) \tilde{\mu}_{k|k-1}^{(j),i}, \quad (33)$$

where, $\mathcal{J}_{k|k-1}$ and n_c are the number of GIW components and target classes obtained by the prediction step, respectively. $w_{k|k-1}^{(j),i}$ is the weight of the jth GIW component of target class i. $\tilde{\mu}_{k|k-1}^{(j),i}$ is the probability of the jth GIW component of target class i. The GIW components obtained by prediction step consist of components of the birth targets $\mathcal{S}_{k|k-1,\mathrm{B}}(\xi)$ and existing targets $\mathcal{S}_{k|k-1,\mathrm{S}}(\xi)$.

The predicted GIW components corresponding to birth targets $\mathcal{S}_{k|k-1,\mathrm{B}}(\xi)$ are:

$$\mathcal{S}_{k|k-1,\mathrm{B}}(\xi) = \sum_{j=1}^{\beta_k} \sum_{i=1}^{n_\mathrm{B}} w_{k|k-1,\mathrm{B}}^{(j),i} \mathcal{N}(\boldsymbol{x}; \boldsymbol{m}_{k|k-1,\mathrm{B}}^{(j),i}, P_{k|k-1,\mathrm{B}}^{(j),i} \otimes X) \times \mathcal{IW}(X; v_{k|k-1,\mathrm{B}}^{(j),i}, V_{k|k-1,\mathrm{B}}^{(j),i}) \tilde{\mu}_{k|k-1,\mathrm{B}}^{(j),i}, \quad (34)$$

with

$$w_{k|k-1,\mathrm{B}}^{(j),i} = \frac{p_\mathrm{B}(1-q_{k-1})}{q_{k|k-1}} w_{k,\mathrm{B}}^{(j),i}, \ \tilde{\mu}_{k|k-1,\mathrm{B}}^{(j),i} = \tilde{\mu}_{k,\mathrm{B}}^{(j),i}, \quad (35)$$

$$\boldsymbol{m}_{k|k-1,\mathrm{B}}^{(j),i} = \boldsymbol{m}_{k-1,\mathrm{B}}^{(j),i}, \quad P_{k|k-1,\mathrm{B}}^{(j),i} = P_{k-1,\mathrm{B}}^{(j),i}, \quad (36)$$

$$v_{k|k-1,\mathrm{B}}^{(j),i} = v_{k-1,\mathrm{B}}^{(j),i}, \quad V_{k|k-1,\mathrm{B}}^{(j),i} = V_{k-1,\mathrm{B}}^{(j),i}. \quad (37)$$

The predicted GIW components corresponding to existing targets $\mathcal{S}_{k|k-1,\mathrm{S}}(\xi)$ are:

$$\mathcal{S}_{k|k-1,\mathrm{S}}(\xi) = \sum_{j=1}^{\mathcal{J}_{k-1}} \sum_{i=1}^{n_c} w_{k|k-1,\mathrm{S}}^{(j),i} \mathcal{N}(\boldsymbol{x}; \boldsymbol{m}_{k|k-1,\mathrm{S}}^{(j),i}, P_{k|k-1,\mathrm{S}}^{(j),i} \otimes X) \times \mathcal{IW}(X; v_{k|k-1,\mathrm{S}}^{(j),i}, V_{k|k-1,\mathrm{S}}^{(j),i}) \tilde{\mu}_{k|k-1,\mathrm{S}}^{(j),i}, \quad (38)$$

with

$$w_{k|k-1,\mathrm{S}}^{(j),i} = \frac{p_\mathrm{S} q_{k-1}}{q_{k|k-1}} w_{k-1}^{(j),i}, \quad \tilde{\mu}_{k|k-1,\mathrm{S}}^{(j),i} = \tilde{\mu}_{k-1}^{(j),i}, \quad (39)$$

$$\boldsymbol{m}_{k|k-1,\mathrm{S}}^{(j),i} = (F_{k|k-1} \otimes I_d) \boldsymbol{m}_{k-1}^{(j),i}, \quad (40)$$

$$P_{k|k-1,\mathrm{S}}^{(j),i} = Q_{k|k-1} + F_{k|k-1} P_{k-1}^{(j),i} F_{k|k-1}^\mathrm{T}, \quad (41)$$

$$v_{k|k-1,\mathrm{S}}^{(j),i} = \frac{2\delta_k \left(\lambda_{k-1}^{(j),i}+1\right)\left(\lambda_{k-1}^{(j),i}-1\right)\left(\lambda_{k-1}^{(j),i}-2\right)}{\left(\lambda_{k-1}^{(j),i}\right)^2 \left(\lambda_{k-1}^{(j),i}+\delta_k\right)} + 2d + 4, \quad (42)$$

$$V_{k|k-1,\mathrm{S}}^{(j),i} = \frac{\delta_k \left(v_{k|k-1,\mathrm{S}}^{(j),i} - 2d - 2\right)}{\lambda_{k-1}^{(j),i}} A_k V_{k-1}^{(j),i} A_k^\mathrm{T}, \quad (43)$$

$$\lambda_{k-1}^{(j),i} = v_{k-1}^{(j),i} - 2d - 2. \quad (44)$$

The predicted exist probability is

$$q_{k|k-1} = p_\mathrm{B}(1-q_{k-1}) + p_\mathrm{S} q_{k-1}. \quad (45)$$

Since the target class of the birth target is known, the number of target class in (33) is still n_c (i.e., the same as in (31)). Based on (34) and (38), we have $\mathcal{J}_{k|k-1} = \mathcal{J}_{k-1} + \beta_k$.

2) UPDATE STEP

Under linear Gaussian assumption as (4) and the measurement noise model as (6), the updated spatial distribution is also a mixture of GIW

$$\mathcal{S}_k(\xi) = \sum_{j=1}^{\mathcal{J}_k} \sum_{i=1}^{n_c} w_k^{(j),i} \mathcal{N}(\boldsymbol{x}; \boldsymbol{m}_k^{(j),i}, P_k^{(j),i} \otimes X) \times \mathcal{IW}(X; v_k^{(j),i}, V_k^{(j),i}) \tilde{\mu}_k^{(j),i}, \quad (46)$$

where, $\mathcal{J}_k$ and n_c are the number of GIW components and target classes obtained by the update step, respectively. $w_k^{(j),i}$ is the weight of the jth GIW component of target class i. $\tilde{\mu}_k^{(j),i}$ is the probability of the jth GIW component of target class i. The GIW components obtained by update step consist of components of the non-detection case $\mathcal{S}_{k,\mathrm{ND}}(\xi)$ and detection case $\mathcal{S}_{k,\mathrm{D}}(\xi, \boldsymbol{W})$.

The updated GIW components of non-detection case $\mathcal{S}_{k,\mathrm{ND}}(\xi)$ are:

$$\mathcal{S}_{k,\mathrm{ND}}(\xi) = \sum_{j=1}^{\mathcal{J}_{k|k-1}} \sum_{i=1}^{n_c} w_{k,\mathrm{ND}}^{(j),i} \mathcal{N}(\boldsymbol{x}; \boldsymbol{m}_{k,\mathrm{ND}}^{(j),i}, P_{k,\mathrm{ND}}^{(j),i} \otimes X) \times \mathcal{IW}(X; v_{k,\mathrm{ND}}^{(j),i}, V_{k,\mathrm{ND}}^{(j),i}) \tilde{\mu}_{k,\mathrm{ND}}^{(j),i}, \quad (47)$$

with

$$w_{k,\mathrm{ND}}^{(j),i} = \frac{(1-p_{\mathrm{D}})^{l_k}}{1-\Delta_k} w_{k|k-1}^{(j),i}, \quad \tilde{\mu}_{k,\mathrm{ND}}^{(j),i} = \tilde{\mu}_{k|k-1}^{(j),i}, \quad (48)$$

$$\boldsymbol{m}_{k,\mathrm{ND}}^{(j),i} = \boldsymbol{m}_{k|k-1}^{(j),i}, \quad P_{k,\mathrm{ND}}^{(j),i} = P_{k|k-1}^{(j),i}, \quad (49)$$

$$v_{k,\mathrm{ND}}^{(j),i} = v_{k|k-1}^{(j),i}, \quad V_{k,\mathrm{ND}}^{(j),i} = V_{k|k-1}^{(j),i}. \quad (50)$$

Clutter distribution $\mathcal{C}(\boldsymbol{z})$ is a uniform distribution with Poisson average rate λ, and $\beta_{\mathrm{FA},k} = \mathcal{C}(\boldsymbol{z})\lambda$. The updated GIW components of detection case $\mathcal{S}_{k,\mathrm{D}}(\xi, \boldsymbol{W})$ are:

$$\mathcal{S}_{k,\mathrm{D}}(\xi, \boldsymbol{W}) = \sum_{j=1}^{\mathcal{J}_{k|k-1}} \sum_{i=1}^{n_c} w_{k,\mathrm{D}}^{(j,\boldsymbol{W}),i} \mathcal{N}(\boldsymbol{x}; \boldsymbol{m}_{k,\mathrm{D}}^{(j,\boldsymbol{W}),i}, P_{k,\mathrm{D}}^{(j,\boldsymbol{W}),i} \otimes X) \times \mathcal{IW}(X; v_{k,\mathrm{D}}^{(j,\boldsymbol{W}),i}, V_{k,\mathrm{D}}^{(j,\boldsymbol{W}),i}) \tilde{\mu}_{k,\mathrm{D}}^{(j,\boldsymbol{W}),i}, \quad (51)$$

with

$$w_{k,\mathrm{D}}^{(j,\boldsymbol{W}),i} = \frac{1}{1-\Delta_k} \psi_k^{|\boldsymbol{W}|} \beta_{\mathrm{FA},k}^{-|\boldsymbol{W}|} \mathcal{L}_{k,\mathrm{Ber}}^{(j,\boldsymbol{W}),i} w_{k|k-1}^{(j),i}, \quad (52)$$

$$\boldsymbol{m}_{k,\mathrm{D}}^{(j,\boldsymbol{W}),i} = \boldsymbol{m}_{k|k-1}^{(j),i} + \left(\boldsymbol{k}_k^{(j,\boldsymbol{W}),i} \otimes I_d\right) \left(\bar{\boldsymbol{z}}_k^{(\boldsymbol{W})} - H_k \boldsymbol{m}_{k|k-1}^{(j),i}\right), \quad (53)$$

$$P_{k,\mathrm{D}}^{(j,\boldsymbol{W}),i} = P_{k|k-1}^{(j),i} - \boldsymbol{k}_k^{(j,\boldsymbol{W}),i} s_k^{(j,\boldsymbol{W}),i} \left(\boldsymbol{k}_k^{(j,\boldsymbol{W}),i}\right)^{\mathrm{T}}, \quad (54)$$

$$v_{k,\mathrm{D}}^{(j,\boldsymbol{W}),i} = |\boldsymbol{W}| + \delta_k^{p,i} + v_{k|k-1}^{(j),i}, \quad (55)$$

$$V_{k,\mathrm{D}}^{(j,\boldsymbol{W}),i} = V_{k|k-1}^{(j),i} + \delta_k^{p,i} (E_k^i)^{-1} Z^{p,i} (E_k^i)^{-\mathrm{T}} + \left(B_k^{(j),i}\right)^{-1} \bar{Z}_k^{(\boldsymbol{W})} \left(B_k^{(j),i}\right)^{-\mathrm{T}} + N_k^{(j,\boldsymbol{W}),i}, \quad (56)$$

$$\boldsymbol{k}_k^{(j,\boldsymbol{W}),i} = P_{k|k-1}^{(j),i} \boldsymbol{h}_k^{\mathrm{T}} \left(s_k^{(j,\boldsymbol{W}),i}\right)^{-1}, \quad (57)$$

$$s_k^{(j,\boldsymbol{W}),i} = \frac{|B_k^{(j),i}|^{2/d}}{|\boldsymbol{W}|} + \boldsymbol{h}_k P_{k|k-1}^{(j),i} \boldsymbol{h}_k^{\mathrm{T}}, \quad (58)$$

$$N_k^{(j,\boldsymbol{W}),i} = \left(s_k^{(j,\boldsymbol{W}),i}\right)^{-1} \left(\bar{\boldsymbol{z}}_k^{(\boldsymbol{W})} - H_k \boldsymbol{m}_{k|k-1}^{(j),i}\right) \times \left(\bar{\boldsymbol{z}}_k^{(\boldsymbol{W})} - H_k \boldsymbol{m}_{k|k-1}^{(j),i}\right)^{\mathrm{T}}, \quad (59)$$

$$\tilde{\mu}_{k,\mathrm{D}}^{(j,\boldsymbol{W}),i} = (\tilde{\nabla}_k)^{-1} \tilde{\Lambda}_k^{(j,\boldsymbol{W}),i} \tilde{\mu}_{k|k-1}^{(j),i}, \quad \tilde{\nabla}_k = \sum_{i=1}^{n_c} \tilde{\Lambda}_k^{(j,\boldsymbol{W}),i} \tilde{\mu}_{k|k-1}^{(j),i}, \quad (60)$$

$$\tilde{\Lambda}_k^{(j,\boldsymbol{W}),i} = \pi^{-\frac{|\boldsymbol{W}|d}{2}} |\boldsymbol{W}|^{-\frac{d}{2}} \left|s_k^{(j,\boldsymbol{W}),i}\right|^{-\frac{d}{2}} \left|B_k^{(j),i}\right|^{-\frac{|\boldsymbol{W}|-1}{2}} \times (\delta_k^{p,i})^{\frac{\delta_k^{p,i} d}{2}} |Z^{p,i}|^{\frac{\delta_k^{p,i}-d-1}{2}} \Gamma_d^{-1}\left(\frac{\delta_k^{p,i}}{2}\right) \times \left|V_{k|k-1}^{(j),i}\right|^{\frac{v_{k|k-1}^{(j),i}-d-1}{2}} \Gamma_d\left(\frac{v_k^{(j,\boldsymbol{W}),i}-d-1}{2}\right) \times \left|V_k^{(j,\boldsymbol{W}),i}\right|^{-\frac{v_k^{(j,\boldsymbol{W}),i}-d-1}{2}} \Gamma_d^{-1}\left(\frac{v_{k|k-1}^{(j),i}-d-1}{2}\right). \quad (61)$$

where $\bar{\boldsymbol{z}}_k^{(\boldsymbol{W})} = \frac{1}{|\boldsymbol{W}|} \sum_{\boldsymbol{z}_k \in \boldsymbol{W}} \boldsymbol{z}_k$, $\bar{\boldsymbol{Z}}_k^{(\boldsymbol{W})} = \sum_{\boldsymbol{z}_k \in \boldsymbol{W}} \left(\boldsymbol{z}_k - \bar{\boldsymbol{z}}_k^{(\boldsymbol{W})}\right) \left(\boldsymbol{z}_k - \bar{\boldsymbol{z}}_k^{(\boldsymbol{W})}\right)^{\mathrm{T}}$.

The updated existence probability is

$$q_k = \frac{1-\Delta_k}{1-q_{k|k-1}\Delta_k} q_{k|k-1}, \quad (62)$$

$$\Delta_k = 1 - (1-p_{\mathrm{D}})^{l_k} - \sum_{\boldsymbol{W} \in \boldsymbol{P}_{1:l(\boldsymbol{\mathcal{Z}}_k)}} \psi_k^{|\boldsymbol{W}|} \beta_{\mathrm{FA},k}^{-|\boldsymbol{W}|} \times \sum_{j=1}^{\mathcal{J}_{k|k-1}} \sum_{i=1}^{n_c} \mathcal{L}_{k,\mathrm{Ber}}^{(j,\boldsymbol{W}),i} w_{k|k-1}^{(j,\boldsymbol{W}),i}, \quad (63)$$

$$\psi_k^{|\boldsymbol{W}|} = \frac{l_k!}{(l_k - |\boldsymbol{W}|)!} \frac{p_{\mathrm{D}}^{|\boldsymbol{W}|}}{(1-p_{\mathrm{D}})^{|\boldsymbol{W}|-l_k}}, \quad (64)$$

$$\mathcal{L}_{k,\mathrm{Ber}}^{(j,W),i} = \tilde{\Lambda}_k^{(j,\boldsymbol{W}),i}. \quad (65)$$

The number of target classes in (46) is still n_c. Based on (47) and (51), we have $\mathcal{J}_k = \mathcal{J}_{k-1} + n_{\boldsymbol{W}}$, where $n_{\boldsymbol{W}}$ is the number of cells in all partitions. The detailed derivation of (52)-(61) and (63)-(65) can be found in Appendix A, and the pseudo code of he proposed JTC-GIW-Ber filter is given in Appendix B.

B. STATE EXTRACTION, PRUNING, AND MERGING

The proposed JTC-GIW-Ber filter consists of n_c parallel class-dependent GIW-Ber filters. For the state extraction of the JTC-GIW-Ber filter, we first judge whether the target exists or not. For the class-dependent GIW-Ber filters, if $q_k^i \geq 0.5$, we judge that the target exists. Then, the parameters of estimated state can be obtained by maximum a posterior (MAP) criterion, that is, $j^* = \underset{j}{\operatorname{argmax}}\, w_k^{(j),i}$, $\hat{\boldsymbol{m}}_k^i = \boldsymbol{m}_k^{(j^*),i}$, $\hat{P}_k^i = P_k^{(j^*),i}$, $\hat{v}_k^i = v_k^{(j^*),i}$, $\hat{V}_k^i = V_k^{(j^*),i}$, and $\hat{\mu}_k^i = \tilde{\mu}_k^{(j^*),i}$. Because there are n_c parallel class-dependent GIW-Ber filters, we should consider the influence of all filters on target state estimation. Therefore, we use expectation a posterior (EAP) criterion to combine n_c GIW components to represent the final target state at time k. Accordingly, the parameters of GIW components representing the target state are

$$\boldsymbol{m}_k = \sum_{i=1}^{n_c} \hat{\mu}_k^i \hat{\boldsymbol{m}}_k^i, \quad P_k = \sum_{i=1}^{n_c} \hat{\mu}_k^i \hat{P}_k^i, \quad (66)$$

$$v_k = \sum_{i=1}^{n_c} \hat{\mu}_k^i \hat{v}_k^i, \quad V_k = \sum_{i=1}^{n_c} \hat{\mu}_k^i \hat{V}_k^i. \quad (67)$$

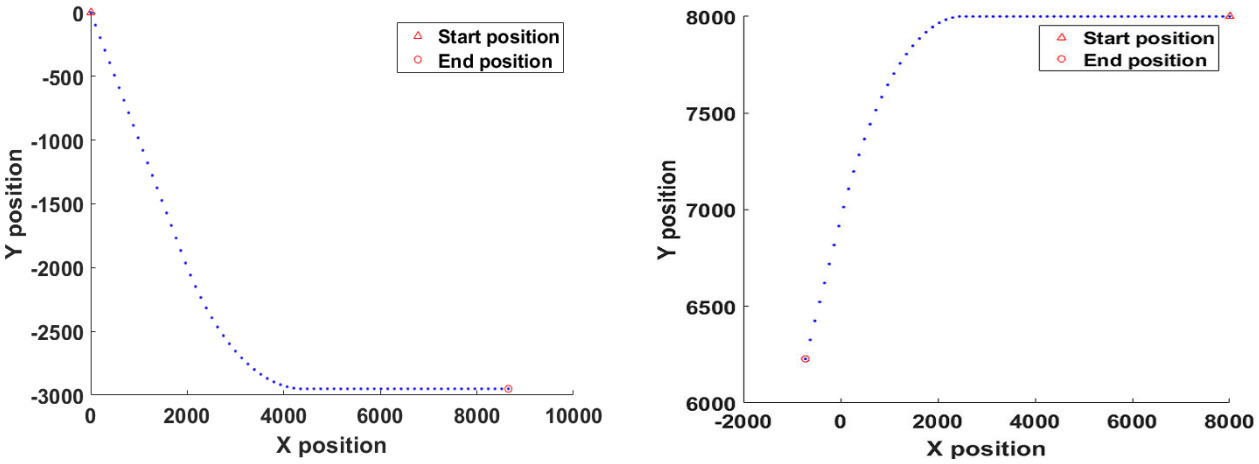

FIGURE 1. True trajectory of target centroid. (a) Simulation scenario 1 and (b) simulation scenario 2.

Ultimately, the final estimates of kinematic state x_k and extent state X_k are

$$\hat{\boldsymbol{x}}_k = \boldsymbol{m}_k, \hat{X}_k = V_k/(v_k - 2d - 2). \tag{68}$$

The target class is determined by probability $\hat{\mu}_k^i$.

The number of GIW components in the proposed JTC-GIW-Ber filter will grow exponentially. Therefore, proper pruning and merging strategy should be considered, as those adopted in [30].

IV. SIMULATION RESULTS

A. PARAMETERS SETTING

In this section, we use the simulated data to test our proposed method and similar application scenarios as those in [1] are considered. Simulation experiments are carried out to illustrate effectiveness of the proposed JTC-GIW-Ber filter in improving the estimation of extent state and obtaining the accurate classification. We compare the proposed JTC-GIW-Ber filter with the JTC-GIW-PHD filter [19] and the GIW-Ber filter [30] in tracking performance. We also compare the proposed JTC-GIW-Ber filter with the JTC-GIW-PHD filter in classification function. To indicate that JTC methods, rather than target tracking methods, can improve the results of target estimation (i.e., target tracking), we use the same RMM as that adopted by Lan and Li [11] in the GIW-Ber filter, and the resulting method is referred to as the improved GIW-Ber filter. In the following text, the improved GIW-Ber filter (denoted as GIW-Ber filter for concision) is used for comparative experiments.

The simulation duration is 100 and the sampling time is $t_s = 10$s. For extended targets, as the range increases (decreases) over time, a target may occupy fewer (more) number of resolution cells. Therefore, the number of target-originated measurements and the detected target size reduce (increase). There are two time-varying simulation scenarios in this paper. The Nimitz-class aircraft carrier (target class 1) and Oliver Hazard Perry class frigate (target class 2) are used in simulation scenario 1, and the Nimitz-class aircraft carrier (target class 1) and Yamato (target class 3) are used in simulation scenario 2. The prior size information of the targets are described by SPD random matrix $Z^{p,1}$, $Z^{p,2}$, and $Z^{p,3}$,

$$Z^{p,1} = \begin{bmatrix} 170^2 & 0 \\ 0 & 40^2 \end{bmatrix} \mathrm{m}^2, \quad Z^{p,2} = \begin{bmatrix} 70^2 & 0 \\ 0 & 7.5^2 \end{bmatrix} \mathrm{m}^2,$$
$$Z^{p,3} = \begin{bmatrix} 132^2 & 0 \\ 0 & 20^2 \end{bmatrix} \mathrm{m}^2. \tag{69}$$

In the two simulation scenarios, the radar sensor is located at $[10, 10]^{\mathrm{T}}$m. The surveillance areas of two simulation scenarios are 10000m × 6000m and 9000m × 2000m, respectively. Simulation scenario 1 describes a target moving far away from the sensor from the initial position $[0, 0]^{\mathrm{T}}$m. While simulation scenario 2 describes a target moving close to the sensor from the initial position $[8000, 8000]^{\mathrm{T}}$m. This paper proposes JTC-GIW-Ber filter for single extended target. The turn tracks considers target maneuvering and non-maneuvering, and it is effective to test the performance of the proposed JTC-GIW-Ber filter. Fig. 1 shows the true trajectory of target centroid of two simulation scenarios.

For simulation scenario 1, the received target size and number of measurements linearly decrease. Targets are born at time $k = 15$ and die at time $k = 85$. For target class 1, the extent state is reduced from $(170, 40)$m to $(150, 30)$m over time. The true number of measurements $l_{k,\mathrm{true}}$ is reduced from 30 to 20 over time. For target class 2, the extent state is reduced from $(70, 7.5)$m to $(50, 5.5)$m over time. The true number of measurements $l_{k,\mathrm{true}}$ is reduced from 20 to 15 over time.

For simulation scenario 2, the received target size and number of measurements linearly increase. Targets are born at time $k = 5$ and die at time $k = 72$. For target class 1, the extent is increased to $(190, 60)$m from $(170, 40)$m. The

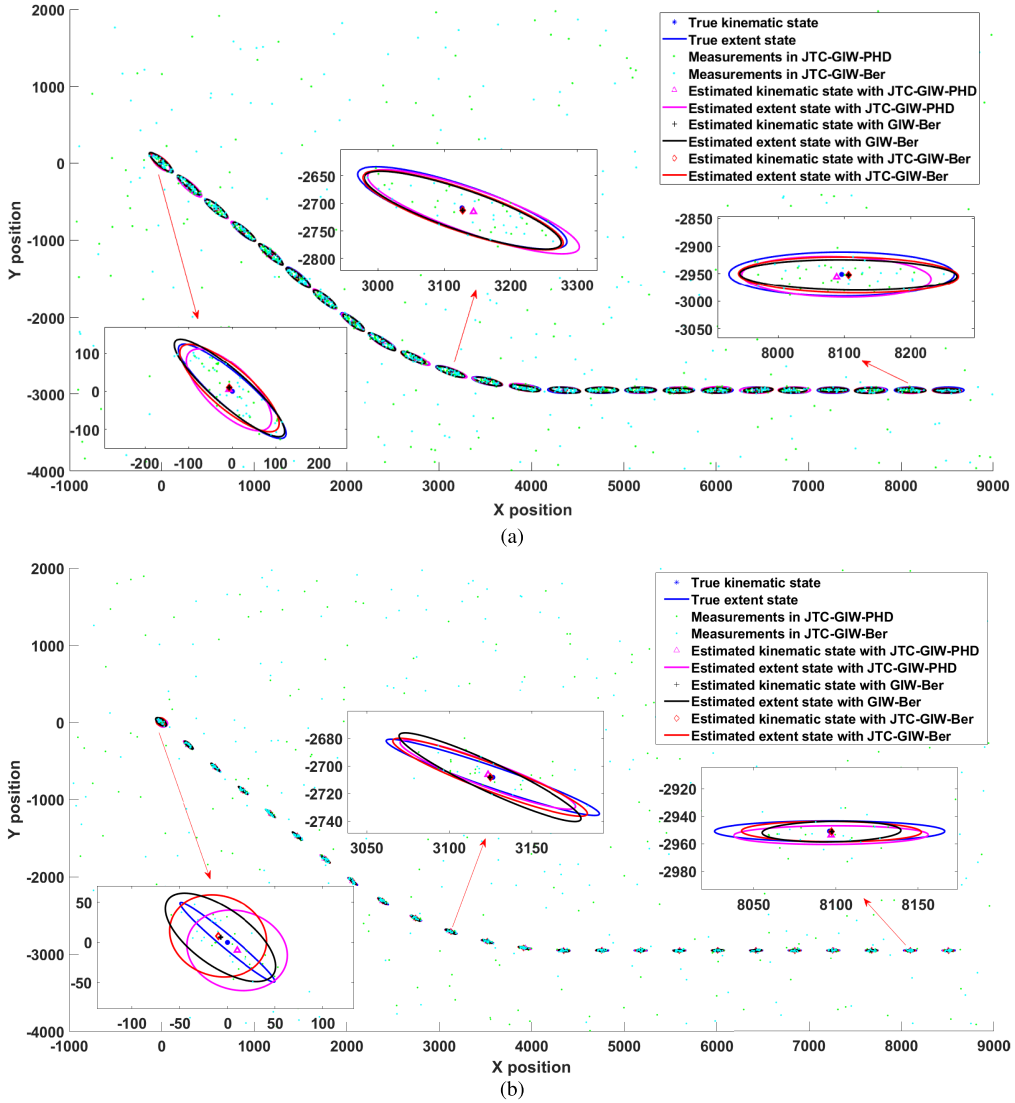

FIGURE 2. The simulation results of target tracking. (a) Target class 1 of simulation scenario 1 and (b) target class 2 of simulation scenario 1.

true number of measurements $l_{k,\text{true}}$ is increased to 35 from 25. For target class 3, the extent is increased to (150, 30)m from (132, 20)m. The true number of measurements $l_{k,\text{true}}$ is increased to 25 over time starting from 20.

The following birth model is used in three filters:

$$\begin{aligned} \boldsymbol{m}_{k,\text{B}}^{(j),i} &= [250\text{m}, 250\text{m}, 3\text{m/s}, 3\text{m/s}, 0, 0]^{\text{T}} \\ P_{k,\text{B}}^{(j),i} &= \text{diag}([10^2\text{m}^2, 10^2\text{m}^2/\text{s}^2, 1^2\text{m}^2/\text{s}^4]) \\ v_{k,\text{B}}^{(j),i} &= 8, \quad V_{k,\text{B}}^{(j),i} = \text{diag}([100^2, 100^2]) \\ n_{\text{B}} &= 1, \quad \mu_{k,\text{B}} = 0.5, \; w_{k,\text{B}}^{(j),i} = 1 \end{aligned} \tag{70}$$

The main parameters of the proposed JTC-GIW-Ber filter, the GIW-Ber filter, and the JTC-GIW-PHD filter are: $p_{\text{S}} = 0.99$, $p_{\text{B}} = 0.01$, $\Sigma = 10^{-3}\text{m}^2/\text{s}$, $\theta = 8t_{\text{s}}$, $B_k = (\eta X_{k|k-1}+R_k)^{1/2}X_{k|k-1}^{-1/2}$, $\eta = 1/4$, $R_k = \text{diag}([10^2, 10^2])\text{m}^2$, $X_{k|k-1} = V_{k|k-1}/(v_{k|k-1} - 2d - 2)$, $\delta_k = 5$, $A_k = \delta_k^{1/2}I_d$, $P_0 = \text{diag}([10^2\text{m}^2, 10^2\text{m}^2/\text{s}^2, 1\text{m}^2/\text{s}^4])$, $v_0 = 8$, and $V_0 = (v_0 - 2d - 2)\text{diag}([100^2, 100^2])$. For simulation scenario 1, $\boldsymbol{m}_0 = [0, 0, 15\text{m/s}, -15\text{m/s}, 0, 0]^{\text{T}}$. For simulation scenario 2, $\boldsymbol{m}_0 = [7600\text{ m}, 7600\text{m}, -15\text{m/s}, 2\text{m/s}, 0, 0]^{\text{T}}$. The truncation threshold for weights is $t_{\text{trunc}} = 10^{-4}$, the merging threshold is $u = 20$, and the maximum allowable number of GIW mixture is $\alpha_{\max} = 100$. Clustering of the received measurements is obtained by the distance partitioning method.

B. SIMULATION RESULTS

To demonstrate the effectiveness of the proposed JTC-GIW-Ber filter, the simulation results are given in terms of target tracking and target classification. For target tracking, we compare the proposed JTC-GIW-Ber filter with the GIW-Ber filter and the JTC-GIW-PHD filter. For target classification, we compare the proposed JTC-GIW-Ber filter with the JTC-GIW-PHD filter. We also give an evaluation of the algorithm complexity.

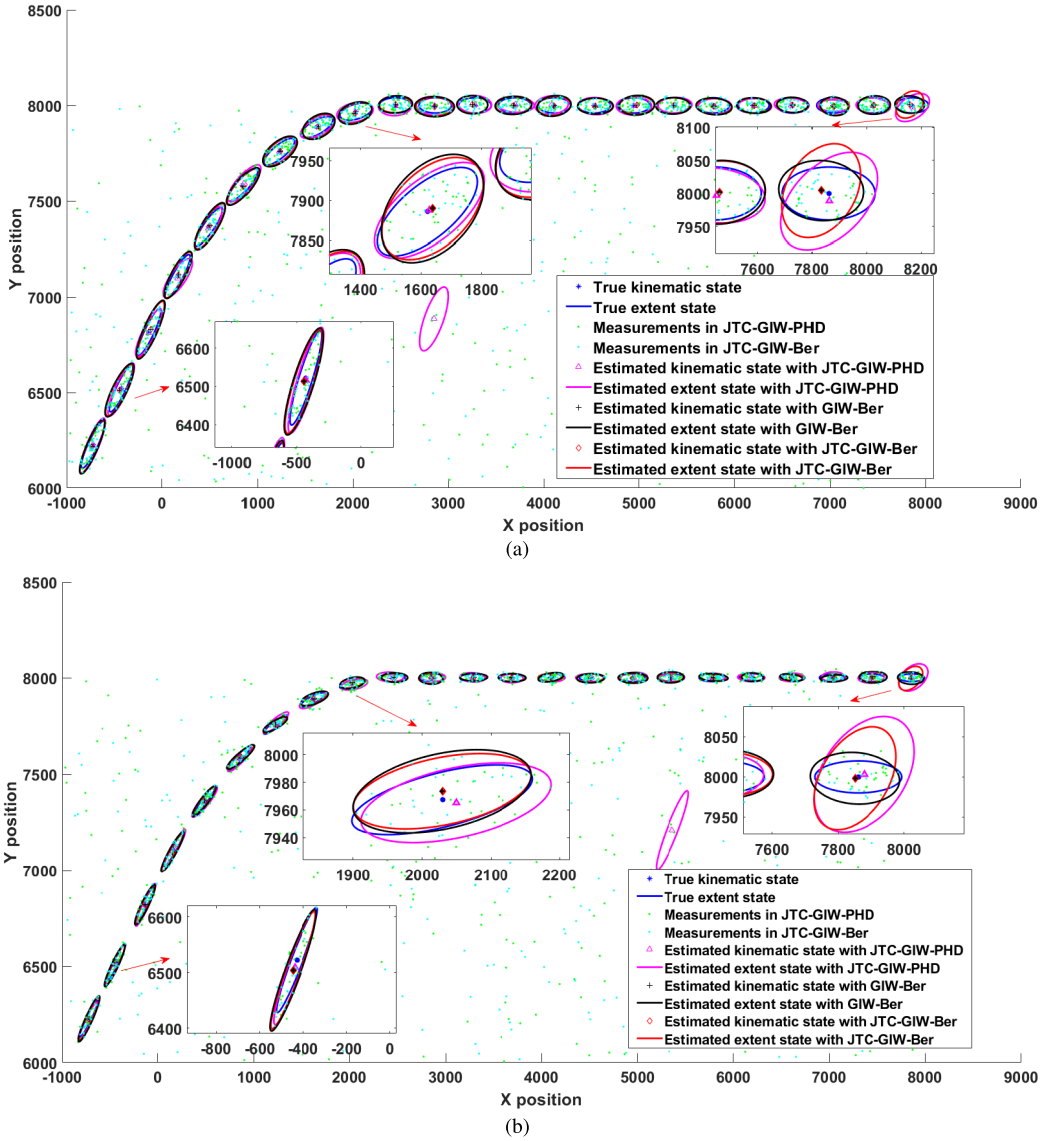

FIGURE 3. The simulation results of target tracking. (a) Target class 1 of simulation scenario 2 and (b) target class 3 of simulation scenario 2.

1) SIMULATION RESULTS FOR TARGET TRACKING

Firstly, we qualitatively evaluate the performance of the proposed JTC-GIW-Ber filter, the GIW-Ber filter, and the JTC-GIW-PHD filter. For the convenience of comparison, Fig. 2 and Fig. 3 present the simulation results of two simulation scenarios at sampling times divisible by 3 when the target exists. The clutter is uniformly distributed over the surveillance area with average clutter rate $\lambda = 10$ and the probability of detection is $p_{\mathrm{D}} = 0.98$. Fig. 2(a) and Fig. 2(b) show the simulation results of target class 1 and 2 for simulation scenario 1, and Fig. 3(a) and Fig. 3(b) show the simulation results of target class 1 and 3 for simulation scenario 2. As shown in Fig. 2 and Fig. 3, the estimated kinematic state of the proposed JTC-GIW-Ber filter is the same as that of the GIW-Ber filter, since the positions of black points closely coincide with red points. The estimated extent state of the proposed JTC-GIW-Ber filter is better than that of the GIW-Ber filter, as shown that the red ellipse is larger than the black ellipse in Fig. 2. The estimated extent state of the proposed JTC-GIW-Ber filter is better than that of the GIW-Ber filter, as shown that the red ellipse is smaller than the black ellipse in Fig. 3. These indicate that the proposed JTC-GIW-Ber filter can achieve better performance in estimating time-varying extent state compared with the GIW-Ber filter. However, the proposed JTC-GIW-Ber filter and the JTC-GIW-PHD filter have similar performance in estimating the extent state, as the red ellipse is similar to the magenta ellipse. But the estimation of cardinality of the JTC-GIW-PHD filter has larger error, as shown that the target is overestimated in Fig. 3.

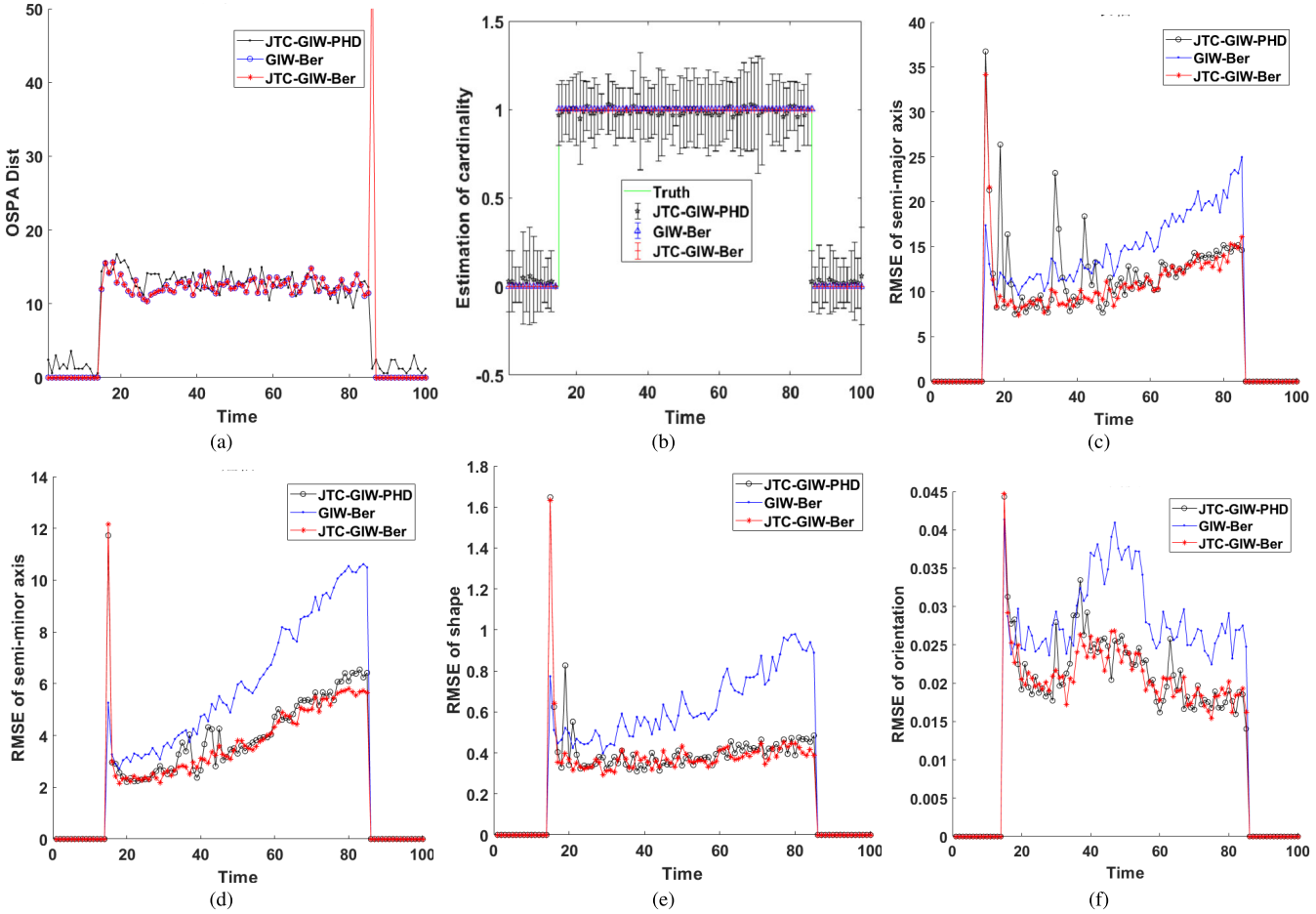

FIGURE 4. Tracking results of target class 1 in simulation scenario 1. (a) OSPA of localization and cardinality error, (b) cardinality estimation mean and standard deviation, (c) RMSE of semi-major axis, (d) RMSE of semi-minor axis, (e) RMSE of shape, and (f) RMSE of orientation angle.

TABLE 2. The tracking effects of two filters under different average clutter rates λ and probabilities of detection P_D for target class 1 in simulation scenario 1.

		$\lambda=10$ $P_D=0.98$	$\lambda=20$ $P_D=0.98$	$\lambda=30$ $P_D=0.98$	$\lambda=10$ $P_D=0.88$	$\lambda=10$ $P_D=0.78$
Semi-major axis (m)	JTC-GIW-PHD	7.75	9.24	16.54	8.77	8.51
	GIW-Ber	10.40	10.40	10.44	10.72	11.25
	JTC-GIW-Ber	7.92	7.94	7.93	7.96	8.11
Semi-minor axis (m)	JTC-GIW-PHD	2.81	3.16	4.75	2.93	2.89
	GIW-Ber	4.25	4.20	4.22	4.38	4.30
	JTC-GIW-Ber	2.79	2.76	2.76	2.77	2.62
Shape	JTC-GIW-PHD	0.28	0.30	0.39	0.30	0.30
	GIW-Ber	0.44	0.44	0.44	0.45	0.46
	JTC-GIW-Ber	0.28	0.28	0.28	0.28	0.28
Orientation (rad)	JTC-GIW-PHD	0.0142	0.0169	0.0248	0.0155	0.0160
	GIW-Ber	0.0198	0.0201	0.0197	0.0206	0.0220
	JTC-GIW-Ber	0.0147	0.0150	0.0148	0.0151	0.0156
Cardinality	JTC-GIW-PHD	0.0147	0.0264	0.0203	0.0123	0.0048
	GIW-Ber	0	0	0	0	0
	JTC-GIW-Ber	0	0	0	0	0
OSPA	JTC-GIW-PHD	11.13	11.99	14.29	9.64	9.75
	GIW-Ber	8.50	8.46	8.57	9.47	9.61
	JTC-GIW-Ber	8.49	8.45	8.56	9.47	9.61

For quantitative evaluation, we compare the proposed JTC-GIW-Ber filter with the GIW-Ber filter and the JTC-GIW-PHD filter. The performance of three filters are evaluated via 100 Monte Carlo simulations. We use the optimal subpattern assignment (OSPA) [31] to measure the error sum of localization and cardinality error with cut-off

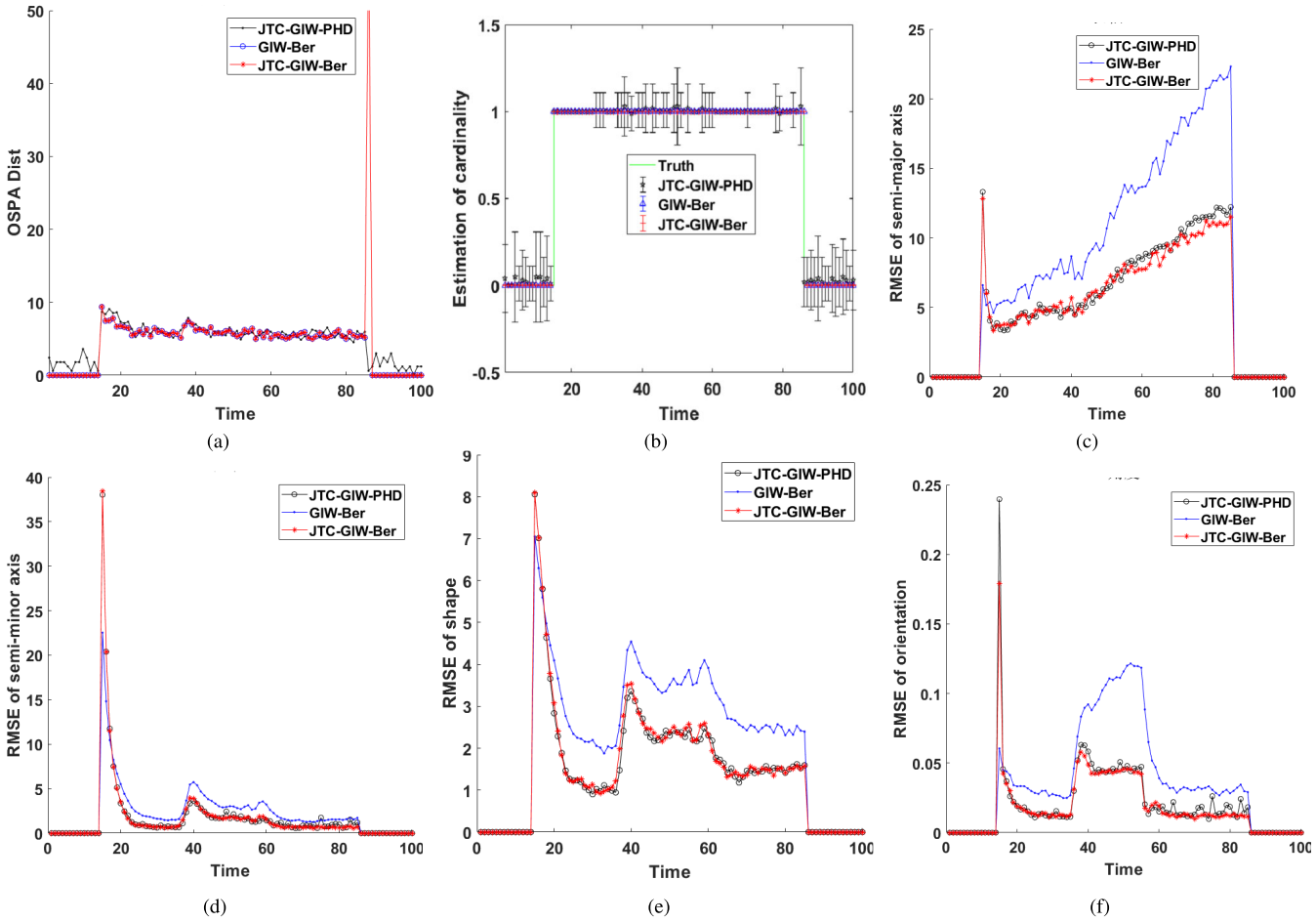

FIGURE 5. Tracking results of target class 2 in simulation scenario 1. (a) OSPA of localization and cardinality error, (b) cardinality estimation mean and standard deviation, (c) RMSE of semi-major axis, (d) RMSE of semi-minor axis, (e) RMSE of shape, and (f) RMSE of orientation angle.

TABLE 3. The tracking effects of two filters under different average clutter rates λ and probabilities of detection P_D for target class 2 in simulation scenario 1.

		$\lambda=10$ $P_D=0.98$	$\lambda=20$ $P_D=0.98$	$\lambda=30$ $P_D=0.98$	$\lambda=10$ $P_D=0.88$	$\lambda=10$ $P_D=0.78$
Semi-major axis (m)	JTC-GIW-PHD	5.73	6.70	10.14	5.21	5.11
	GIW-Ber	8.33	8.25	8.32	8.47	8.65
	JTC-GIW-Ber	5.17	5.13	5.16	5.05	4.91
Semi-minor axis (m)	JTC-GIW-PHD	1.92	2.56	4.22	1.73	1.75
	GIW-Ber	2.11	2.17	2.18	2.26	2.36
	JTC-GIW-Ber	1.62	1.67	1.66	1.68	1.72
Shape	JTC-GIW-PHD	1.51	1.58	1.72	1.48	1.47
	GIW-Ber	2.13	2.19	2.19	2.24	2.30
	JTC-GIW-Ber	1.48	1.52	1.52	1.51	1.50
Orientation (rad)	JTC-GIW-PHD	0.0204	0.0242	0.0323	0.0201	0.0210
	GIW-Ber	0.0371	0.0380	0.0366	0.0378	0.0406
	JTC-GIW-Ber	0.0183	0.0186	0.0181	0.0183	0.0192
Cardinality	JTC-GIW-PHD	0.0074	0.0228	0.0597	0.0062	0.0061
	GIW-Ber	0	0	0	0	0
	JTC-GIW-Ber	0	0	0	0	0
OSPA	JTC-GIW-PHD	4.54	6.29	9.50	4.75	5.07
	GIW-Ber	3.98	3.96	4.01	4.79	4.47
	JTC-GIW-Ber	3.98	3.95	4.01	4.79	4.47

parameter $c = 60$ and $p = 2$. For the evaluation of target shape, four root mean square error (RMSE) parameters: semi-major axes length, semi-minor axes length, shape (ratio of major and minor axes), and orientation angle are used to evaluate the performance of three filters. The semi-major axes length, semi-minor axes length, and orientation angle

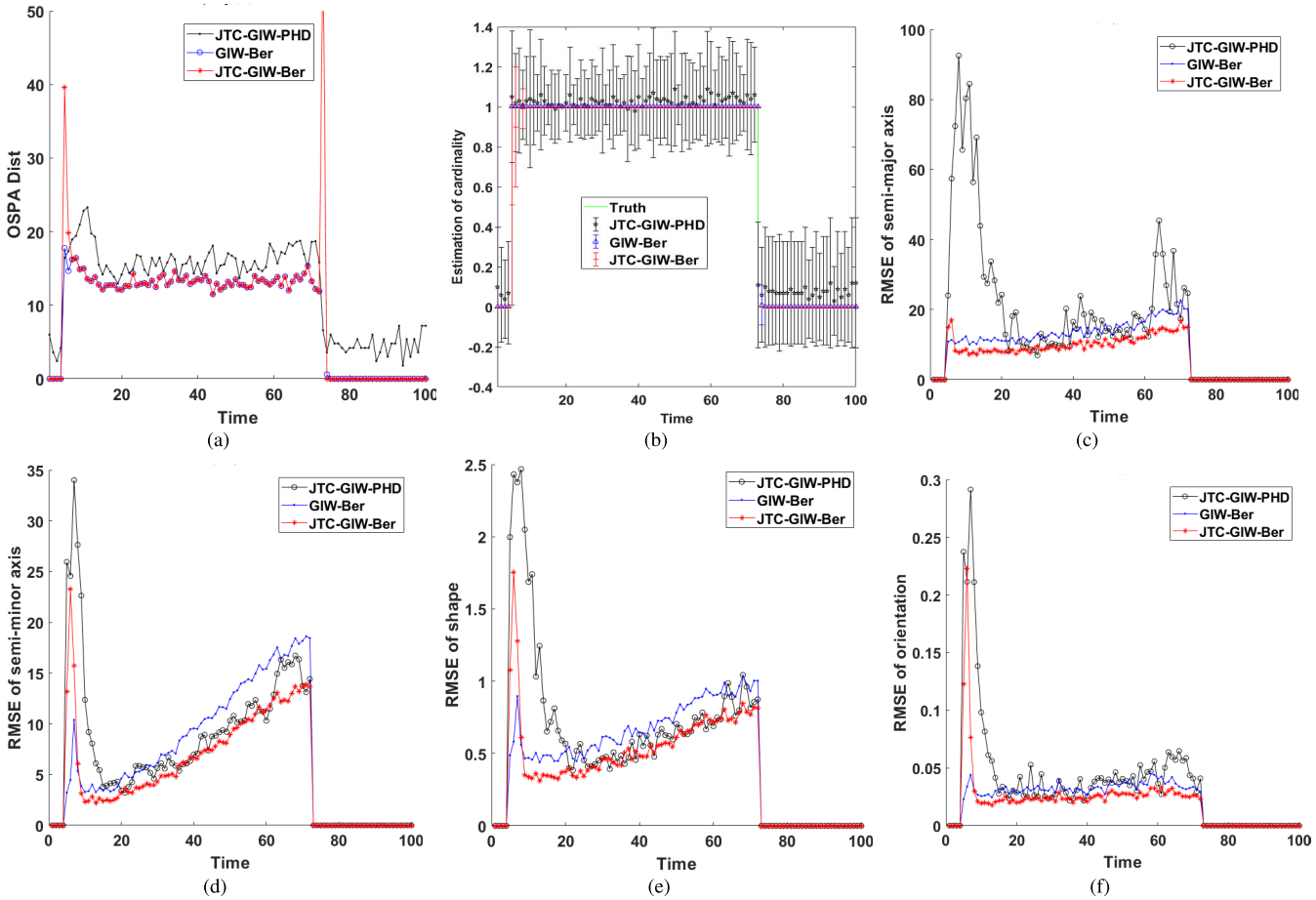

FIGURE 6. Tracking results of target class 1 in simulation scenario 2. (a) OSPA of localization and cardinality error, (b) cardinality estimation mean and standard deviation, (c) RMSE of semi-major axis, (d) RMSE of semi-minor axis, (e) RMSE of shape, and (f) RMSE of orientation angle.

TABLE 4. The tracking effects of two filters under different average clutter rates λ and probabilities of detection P_D for target class 1 in simulation scenario 2.

		$\lambda=10$ $P_D=0.98$	$\lambda=20$ $P_D=0.98$	$\lambda=30$ $P_D=0.98$	$\lambda=10$ $P_D=0.88$	$\lambda=10$ $P_D=0.78$
Semi-major axis (m)	JTC-GIW-PHD	16.50	46.88	77.51	16.77	10.77
	GIW-Ber	9.30	8.83	7.75	9.47	9.34
	JTC-GIW-Ber	7.18	6.64	5.88	7.06	6.68
Semi-minor axis (m)	JTC-GIW-PHD	6.88	10.37	14.15	6.86	5.17
	GIW-Ber	6.66	6.56	6.14	6.66	6.64
	JTC-GIW-Ber	5.44	4.95	4.71	5.20	4.80
Shape	JTC-GIW-PHD	0.53	0.89	1.23	0.55	0.45
	GIW-Ber	0.47	0.45	0.41	0.47	0.47
	JTC-GIW-Ber	0.40	0.36	0.34	0.39	0.38
Orientation (rad)	JTC-GIW-PHD	0.0339	0.0626	0.0928	0.0361	0.0271
	GIW-Ber	0.0217	0.0208	0.0179	0.0224	0.0224
	JTC-GIW-Ber	0.0209	0.0160	0.0140	0.0203	0.0180
Cardinality	JTC-GIW-PHD	0.0162	0.0309	0.0619	0.0202	0.0283
	GIW-Ber	0.0002	0.0297	0.1178	0.0060	0.0191
	JTC-GIW-Ber	0.0002	0.0297	0.1178	0.0060	0.0191
OSPA	JTC-GIW-PHD	13.10	21.35	31.59	12.62	12.72
	GIW-Ber	8.52	8.64	8.67	9.69	9.78
	JTC-GIW-Ber	8.52	9.93	14.06	9.95	10.51

can be obtained from the estimated $\hat{X}_k = V_k/(v_k - 2d - 2)$ according to the method in [32]. The average clutter rate is $\lambda = 10$ and the probability of detection is $p_D = 0.88$. The tracking results of simulation scenario 1 are shown in Fig. 4 for target class 1 and Fig. 5 for target class 2, respectively. The tracking results of simulation scenario 2 are shown in Fig. 6 for target class 1 and Fig. 7 for target class 3, respectively.

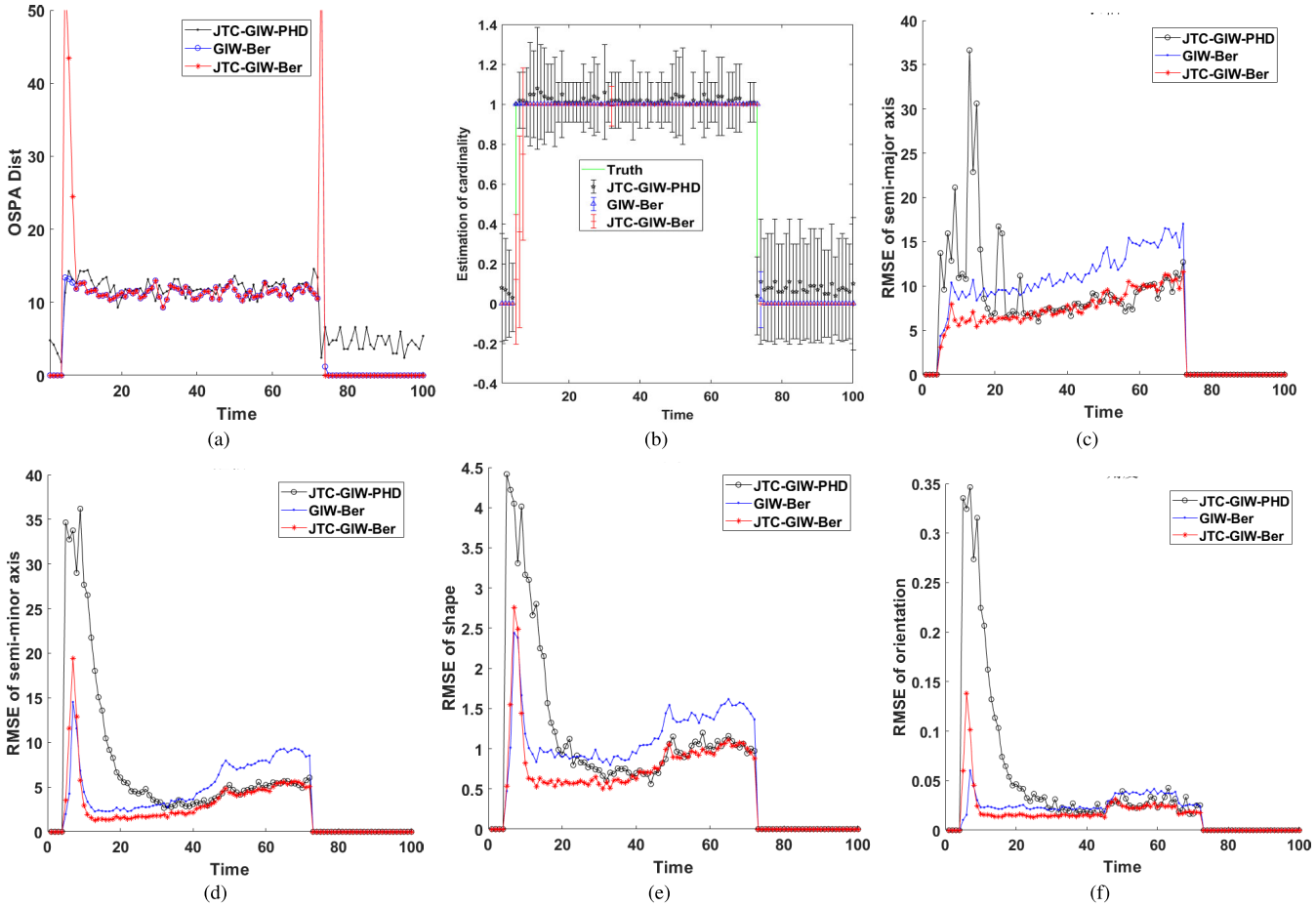

FIGURE 7. Tracking results of target class 3 in simulation scenario 2. (a) OSPA of localization and cardinality error, (b) cardinality estimation mean and standard deviation, (c) RMSE of semi-major axis, (d) RMSE of semi-minor axis, (e) RMSE of shape, and (f) RMSE of orientation angle.

TABLE 5. The tracking effects of two filters under different average clutter rates λ and probabilities of detection P_D for target class 3 in simulation scenario 2.

		$\lambda=10$ $P_D=0.98$	$\lambda=20$ $P_D=0.98$	$\lambda=30$ $P_D=0.98$	$\lambda=10$ $P_D=0.88$	$\lambda=10$ $P_D=0.78$
Semi-major axis (m)	JTC-GIW-PHD	9.34	22.43	46.65	6.92	6.95
	GIW-Ber	7.89	7.42	7.18	7.74	7.52
	JTC-GIW-Ber	5.51	5.15	4.98	5.24	4.93
Semi-minor axis (m)	JTC-GIW-PHD	4.12	5.92	8.82	5.56	2.97
	GIW-Ber	3.91	3.50	3.25	3.69	3.61
	JTC-GIW-Ber	2.99	2.22	2.00	2.50	2.23
Shape	JTC-GIW-PHD	0.73	0.94	1.29	0.88	0.68
	GIW-Ber	0.83	0.76	0.71	0.80	0.78
	JTC-GIW-Ber	0.63	0.53	0.48	0.57	0.53
Orientation (rad)	JTC-GIW-PHD	0.0242	0.0344	0.0548	0.0419	0.0227
	GIW-Ber	0.0183	0.0172	0.0165	0.0189	0.0190
	JTC-GIW-Ber	0.0183	0.0119	0.0112	0.0151	0.0129
Cardinality	JTC-GIW-PHD	0.0119	0.0450	0.1020	0.0190	0.0150
	GIW-Ber	0.0047	0.0304	0.0628	0.0178	0.0294
	JTC-GIW-Ber	0.0047	0.0304	0.0628	0.0178	0.0294
OSPA	JTC-GIW-PHD	9.17	14.77	22.90	9.66	10.15
	GIW-Ber	7.39	7.44	7.47	8.39	8.51
	JTC-GIW-Ber	7.60	8.83	10.38	9.20	9.78

For estimation of kinematic state, the performances of the proposed JTC-GIW-Ber filter and the GIW-Ber filter are almost the same, as shown in Fig. 4(a), Fig. 5(a), Fig. 6(a) and Fig. 7(a). This is due to the fact that no such prior information is used to obtain better performance of the proposed JTC-GIW-Ber filter in the kinematic state estimation. The

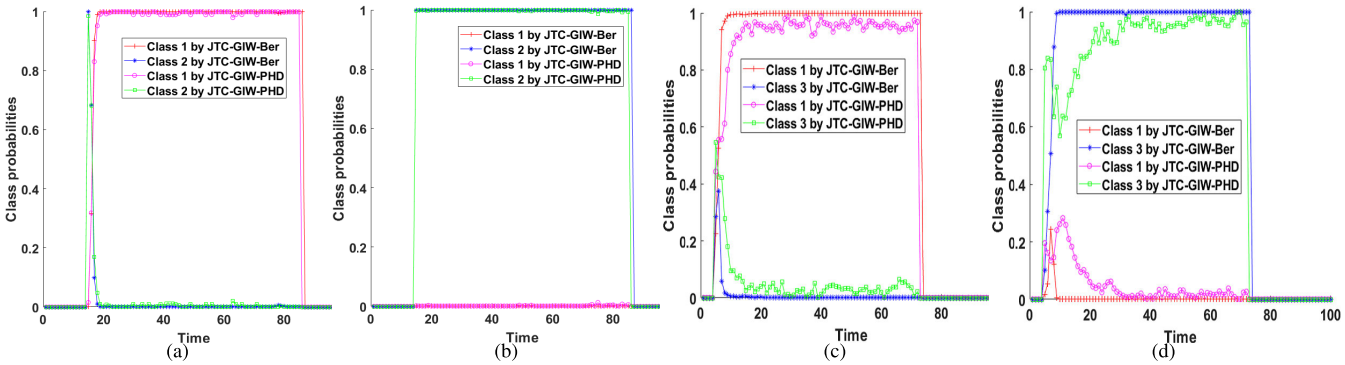

FIGURE 8. The classification results. (a) target class 1 of simulation scenario 1, (b) target class 2 of simulation scenario 1, (c) target class 1 of simulation scenario 2, and (d) target class 3 of simulation scenario 2.

cardinality estimations of the proposed JTC-GIW-Ber and the GIW-Ber are also the same but better than the JTC-GIW-PHD filter, as shown in Fig. 4(b), Fig. 5(b), Fig. 6(b) and Fig. 7(b). It demonstrates that Bernoulli filter is an unbiased filter in cardinality estimation.

For estimation of extent state, the proposed JTC-GIW-Ber filter exhibits better except for the first one or two moments, as shown in Fig. 4(c)-(f), Fig. 5(c)-(f), Fig. 6(c)-(f) and Fig. 7(c)-(f). Especially, the improvement in estimating the semi-major, semi-minor and shape is obvious. The key reason is that we only use the prior information of size and shape, while the prior orientation angle information is not used.

Table 2-Table 5 show the tracking effects of three filters under different average clutter rates λ and probabilities of detection P_{D}. In this paper, the extent state is described by four parameters: semi-major axis, semi-minor axis, shape, and orientation. For a more intuitive understanding, we do not analyze the shape which is decided by the ratio of semi-major axis and semi-minor axis. Compared with the true size of extended targets, different clutter rates λ and detection rates P_{D} hardly affect the estimation result of extent state. For example, for target class 1 of simulation scenario 1, the RMSE of semi-major axis and semi-minor axis at each sample time is about 8m and 2.8m, respectively, as shown in Table 2. Compared with 170m and 40m, the change of about 0.2m and 0.2m can almost be negligible. As for orientation, by taking target class 2 in simulation scenario 1 as an example in Table 3, the RMSE of orientation at each sample time is about 0.012rad. However, the different average clutter rates λ and probabilities of detection P_{D} effect the estimation of cardinality. The higher average clutter rates λ and lower probabilities of detection P_{D} will result in a larger error in estimation of cardinality. The estimation of cardinality will ultimately affect the calculation of OSPA.

Table 2-Table 5 also show that the proposed JTC-GIW-Ber filter has the best performance in the three filters. Because the proposed JTC-GIW-Ber filter only uses the prior size information, it only obviously improves the estimation of extent state compared with the GIW-Ber filter. As for cardinality and OSPA, it almost has the same performance as the GIW-Ber filter.

2) SIMULATION RESULTS FOR TARGET CLASSIFICATION

For classification, results of the two simulation scenarios are shown in Fig. 8. Fig. 8(a) and Fig. 8(b) are the classification results of target class 1 and 2 for simulation scenario 1, respectively. Fig. 8(c) and Fig. 8(d) are the classification results of target class 1 and 3 for simulation scenario 2, respectively. From Fig. 8, it is seen that the class probability estimated by the proposed JTC-GIW-Ber filter is almost equal to 1 or 0, meaning that it has better classification performance than the JTC-GIW-PHD filter.

In a word, the proposed JTC-GIW-Ber filter performs better than the GIW-Ber filter and the JTC-GIW-PHD filter in estimating the extent state, and it can obtain more accurate classification than the JTC-GIW-PHD filter.

3) ALGORITHM COMPLEXITY ANALYSIS

Similar to the GM-PHD filter [33], the GIW-Ber filter requires $\mathcal{O}_{\text{GIW-Ber}}(\mathcal{J}_{k-1}|\mathbf{Z}_k|) = (\mathcal{J}_{k-1} + \beta_k)(1 + n_{\boldsymbol{W}})$. For the proposed JTC-GIW-Ber filter, there are n_c parallel class-dependent GIW-Ber filters. So, it has higher algorithm complexity than the GIW-Ber filter, that is, $\mathcal{O}_{\text{JTC-GIW-Ber}}(\mathcal{J}_{k-1}|\mathbf{Z}_k|) = n_c(\mathcal{J}_{k-1} + \beta_k)(1 + n_{\boldsymbol{W}})$. In this paper, the simulation is conducted with MATLAB R2018a, and all experiments are performed on a computer with one 3.60 GHz Intel(R) Core(TM) i7-7700 8 core CPU and 16 GB RAM. We use MATLAB function tic and toc to obtain the running time. For the target class 1 in simulation scenario 1, average running time of the proposed JTC-GIW-Ber filter and GIW-Ber filter are 4.12s and 2.41s, respectively. Due to the accuracy of the time measurement of the MATLAB function, the $4.12/2.41 \approx 1.71$ shows that the proposed JTC-GIW-Ber filiter has higher algorithm complexity than the GIW-Ber filter. However, we can use parallel operation to meet the requirements of real time processing.

V. CONCLUSION

In this paper, we proposed JTC-GIW-Ber filter to improve the extent state estimation of an extended target by using the prior size information in time-varying and clutter scenarios, and to simultaneously obtain the accurate target classification. The RMM and Bernoulli filter used in this paper can not only estimate the kinematic and extent states, but also achieve

the target classification. Considering the clutter environment, only the single target case is considered. In the future, issues of maneuvering targets and multi-target joint tracking and classification will be further investigated.

APPENDIX A
THE DETAILED DERIVATION OF (52)-(61) AND (63)-(65)

In [11], the PDF of measurements noise is $\boldsymbol{e}_k^m \sim \mathcal{N}\left(0, B_k X_k (B_k)^{\mathrm{T}}\right)$. In order to describe the difference in measurement noise R_k and extent state X_k effects on measurement likelihood function, the $B_k X_k (B_k)^{\mathrm{T}}$ is rewritten as $\eta X_k + R_k$. By using the Cholesky Factorization, we can obtain $B_k = (\eta \bar{X}_{k|k-1} + R_k)^{1/2} (\bar{X}_{k|k-1})^{-1/2}$, and $\bar{X}_{k|k-1}$ is the expectation of $X_{k|k-1}$. The proofs of (52)-(61) and (63)-(65) are derived as follows.

Given the prior information of target class, the partial PDF of detection cases in (14) is

$$\begin{aligned}&\prod_{z_k \in \boldsymbol{W}} \frac{g_k(z|\xi)}{\lambda c(z_k)} \mathcal{S}_{k|k-1}(\xi) \\ &= \beta_{\mathrm{FA},k}^{-|\boldsymbol{W}|} \left\{ \prod_{z_k \in \boldsymbol{W}} \mathcal{N}\left(z_k; (\boldsymbol{h}_k \otimes I_d)\boldsymbol{x}_k, B_k X_k (B_k)^{\mathrm{T}}\right) \right\} \\ &\quad \times \mathcal{W}(Z^{p,i}; \delta_k^{p,i}, E_k^i X_k (E_k^i)^T / \delta_k^{p,i}) \mathcal{S}_{k|k-1}(\xi), \end{aligned} \tag{71}$$

where $\beta_{\mathrm{FA},k} = \lambda \mathcal{C}(\boldsymbol{z})$. The second and third factors on the right side of (71) yield

$$\begin{aligned}&\left\{ \prod_{z_k \in \boldsymbol{W}} \mathcal{N}(z_k; H_k \boldsymbol{x}_k, B_k X_k B_k^{\mathrm{T}}) \right\} \mathcal{W}(Z^{p,i}; \delta_k^{p,i}, E_k^i X_k (E_k^i)^{\mathrm{T}} / \delta_k^{p,i}) \\ &= (2\pi)^{-\frac{|\boldsymbol{W}|d}{2}} \left| B_k X_k B_k^{\mathrm{T}} \right|^{-\frac{|\boldsymbol{W}|}{2}} \mathcal{W}(Z^{p,i}; \delta_k^{p,i}, E_k^i X_k (E_k^i)^{\mathrm{T}} / \delta_k^{p,i}) \\ &\quad \times \mathrm{etr}\left(-\frac{\sum\limits_{z_k \in \boldsymbol{W}} (z_k - H_k \boldsymbol{x}_k)(z_k - H_k \boldsymbol{x}_k)^{\mathrm{T}}}{2} (B_k X_k B_k^{\mathrm{T}})^{-1} \right). \end{aligned} \tag{72}$$

With $\bar{z}_k^{(\boldsymbol{W})} = \frac{1}{|\boldsymbol{W}|} \sum\limits_{z_k \in \boldsymbol{W}} z_k$, $\bar{Z}_k^{(\boldsymbol{W})} = \sum\limits_{z_k \in \boldsymbol{W}} \left(z_k - \bar{z}_k^{(\boldsymbol{W})}\right) \left(z_k - \bar{z}_k^{(\boldsymbol{W})}\right)^{\mathrm{T}}$, and the detailed Wishart PDF, (72) becomes

$$\begin{aligned}&\left\{ \prod_{z_k \in \boldsymbol{W}} \mathcal{N}(z_k; H_k \boldsymbol{x}_k, B_k X_k B_k^{\mathrm{T}}) \right\} \mathcal{W}\left(Z^{p,i}; \delta_k^{p,i}, \frac{E_k^i X_k (E_k^i)^{\mathrm{T}}}{\delta_k^{p,i}}\right) \\ &= 2^{-\frac{(|\boldsymbol{W}|-1+\delta_k^{p,i})d}{2}} \pi^{-\frac{(|\boldsymbol{W}|-1)d}{2}} |X_k|^{-\frac{|\boldsymbol{W}|-1+\delta_k^{p,i}}{2}} |B_k|^{-(|\boldsymbol{W}|-1)} |\boldsymbol{W}|^{-\frac{d}{2}} \\ &\quad \times \Gamma_d^{-1}\left(\frac{\delta_k^{p,i}}{2}\right) (\delta_k^{p,i})^{\frac{\delta_k^{p,i} d}{2}} \left| Z^{p,i} \right|^{\frac{\delta_k^{p,i}-d-1}{2}} \\ &\quad \times \mathcal{N}\left(\bar{z}_k^{(\boldsymbol{W})}; H_k \boldsymbol{x}_k, \frac{B_k X_k B_k^{\mathrm{T}}}{|\boldsymbol{W}|}\right) \\ &\quad \times \mathrm{etr}\left(-\frac{\delta_k^{p,i} (E_k^i)^{-1} Z^{p,i} (E_k^i)^{-\mathrm{T}} X_k^{-1} + B_k^{-1} \bar{Z}_k^{(\boldsymbol{W})} B_k^{-\mathrm{T}} X_k^{-1}}{2} \right). \end{aligned} \tag{73}$$

Combining (31) and (71), we can obtain

$$\begin{aligned}&\beta_{\mathrm{FA},k}^{-|\boldsymbol{W}|} \left\{ \prod_{z_k \in \boldsymbol{W}} \mathcal{N}(z_k; H_k \boldsymbol{x}_k, B_k X_k B_k^{\mathrm{T}}) \right\} \\ &\quad \times \mathcal{W}\left(Z^{p,i}; \delta_k^{p,i}, \frac{E_k^i X_k (E_k^i)^{\mathrm{T}}}{\delta_k^{p,i}}\right) \\ &\quad \left\{ \sum_{j=1}^{\mathcal{J}_{k|k-1}} \sum_{i=1}^{n_{\mathrm{c}}} w_{k|k-1}^{(j),i} \mathcal{N}(\boldsymbol{x}_k; \boldsymbol{m}_{k|k-1}^{(j),i}, P_{k|k-1}^{(j),i} \otimes X_k) \right. \\ &\quad \left. \mathcal{IW}(X_k; v_{k|k-1}^{(j),i}, V_{k|k-1}^{(j),i}) \tilde{\mu}_{k|k-1}^{(j),i} \right\}. \end{aligned} \tag{74}$$

For target tracking, (74) becomes (75) in order to facilitate the derivation and analysis

$$\begin{aligned}&\left\{ \prod_{z_k \in \boldsymbol{W}} \mathcal{N}(z_k; H_k \boldsymbol{x}_k, B_k X_k B_k^{\mathrm{T}}) \right\} \mathcal{W}(Z^{p,i}; \delta_k^{p,i}, E_k^i X_k (E_k^i)^{\mathrm{T}} / \delta_k^{p,i}) \\ &\quad \times \mathcal{N}\left(\boldsymbol{x}_k; \boldsymbol{m}_{k|k-1}^{(j),i}, P_{k|k-1}^{(j),i} \otimes X_k\right) \mathcal{IW}\left(X_k; v_{k|k-1}^{(j),i}, V_{k|k-1}^{(j),i}\right). \end{aligned} \tag{75}$$

Combining (73) and (75), we can obtain (76), shown at the top of the next page.

For two Gaussian factors of (76) as shown at the top of the next page, (77) can be obtained by using $\mathcal{N}(\boldsymbol{x}_2; H\boldsymbol{x}_1, Y_2)\mathcal{N}(\boldsymbol{x}_1; \boldsymbol{y}_1, Y_1) = \mathcal{N}(\boldsymbol{x}_2; H\boldsymbol{y}_1, S)\, \mathcal{N}(\boldsymbol{x}_1; \boldsymbol{y}_1 + K(\boldsymbol{x}_2 - H\boldsymbol{y}_1), Y_1 - KSK^{\mathrm{T}})$ with $K = Y_1 H^{\mathrm{T}} S^{-1}$ and $S = HY_1 H^{\mathrm{T}} + Y_2$ [9].

In (77), $\boldsymbol{m}_k^{(j,\boldsymbol{W}),i} = \boldsymbol{m}_{k|k-1}^{(j),i} + K_k^{(j,W),i}\left(\bar{z}_k^{(\boldsymbol{W})} - H_k \boldsymbol{m}_{k|k-1}^{(j),i}\right)$, $P_k^{(j,\boldsymbol{W}),i} = P_{k|k-1}^{(j),i} - k_k^{(j,\boldsymbol{W}),i} \boldsymbol{h}_k P_{k|k-1}^{(j),i}$, $K_k^{(\boldsymbol{W}),i} = \boldsymbol{k}_k^{(j,\boldsymbol{W}),i} \otimes I_d$, $\boldsymbol{k}_k^{(j,\boldsymbol{W}),i} = P_{k|k-1}^{(j),i} \boldsymbol{h}_k{}^{\mathrm{T}} \left(s_k^{(j,\boldsymbol{W}),i}\right)^{-1}$. To simplify (77), $B_k^{(j),i} X_k \left(B_k^{(j),i}\right)^{\mathrm{T}} \approx \gamma_k X_k$ is adopted, where γ_k is a scalar. By setting the determinants to be identical, i.e., $\left| B_k^{(j),i} X_k \left(B_k^{(j),i}\right)^{\mathrm{T}} \right| = \left|\gamma_k X_k\right|, \gamma_k = |B_k^{(j),i}|^{2/d}$. (77) becomes

$$\begin{aligned}&\mathcal{N}\left(\boldsymbol{x}_k; \boldsymbol{m}_{k|k-1}^{(j),i}, P_{k|k-1}^{(j),i} \otimes X_k\right) \\ &\quad \times \mathcal{N}\left(\bar{z}_k^{(\boldsymbol{W})}; H_k \boldsymbol{x}_k, \frac{B_k^{(j),i} X_k \left(B_k^{(j),i}\right)^{\mathrm{T}}}{|\boldsymbol{W}|}\right) \\ &= \mathcal{N}\left(\boldsymbol{x}_k; \boldsymbol{m}_k^{(j,\boldsymbol{W}),i}, P_k^{(j,\boldsymbol{W}),i} \otimes X_k\right) \\ &\quad \times \mathcal{N}\left(\bar{z}_k^{(\boldsymbol{W})}; H_k \boldsymbol{m}_{k|k-1}^{(j),i}, s_k^{(j,\boldsymbol{W}),i} X_k\right), \end{aligned} \tag{78}$$

where $s_k^{(j,\boldsymbol{W}),i} = \frac{|B_k^i|^{2/d}}{|\boldsymbol{W}|} + \boldsymbol{h}_k P_{k|k-1}^{(j),i} \boldsymbol{h}_k^{\mathrm{T}}$.

By using (78), (76) turns out to be

$$\begin{aligned}&\mathcal{N}\left(\boldsymbol{x}_k; \boldsymbol{m}_k^{(j,\boldsymbol{W}),i}, P_k^{(j,\boldsymbol{W}),i} \otimes X_k\right) \\ &\quad \times \mathcal{N}\left(\bar{z}_k^{(\boldsymbol{W})}; H_k \boldsymbol{m}_{k|k-1}^{(j),i}, s_k^{(j,\boldsymbol{W}),i} X_k^i\right) \end{aligned}$$

$$2^{-\frac{(|\boldsymbol{W}|-1+\delta_k^{p,i})d}{2}}\pi^{-\frac{(|\boldsymbol{W}|-1)d}{2}}|X_k|^{-\frac{|\boldsymbol{W}|-1+\delta_k^{p,i}}{2}}\left|B_k^{(j),i}\right|^{-(|\boldsymbol{W}|-1)}|\boldsymbol{W}|^{-\frac{d}{2}}$$
$$\times\Gamma_d^{-1}\left(\frac{\delta_k^{p,i}}{2}\right)(\delta_k^{p,i})^{\frac{\delta_k^{p,i}d}{2}}|Z^{p,i}|^{\frac{\delta_k^{p,i}-d-1}{2}}\mathcal{N}\left(\bar{\boldsymbol{z}}_k^{(\boldsymbol{W})};H_k\boldsymbol{x}_k,\frac{B_k^{(j),i}X_k\left(B_k^{(j),i}\right)^{\mathrm{T}}}{|\boldsymbol{W}|}\right)$$
$$\times\operatorname{etr}\left(-\frac{\delta_k^{p,i}\left(E_k^i\right)^{-1}Z^{p,i}\left(E_k^i\right)^{-\mathrm{T}}X_k^{-1}+\left(B_k^{(j),i}\right)^{-1}\bar{Z}_k^{(\boldsymbol{W})}\left(B_k^{(j),i}\right)^{-\mathrm{T}}X_k^{-1}}{2}\right)$$
$$\times\mathcal{N}\left(\boldsymbol{x}_k;\boldsymbol{m}_{k|k-1}^{(j),i},P_{k|k-1}^{(j),i}\otimes X_k\right)\mathcal{IW}\left(X_k;v_{k|k-1}^{(j),i},V_{k|k-1}^{(j),i}\right)\tag{76}$$

$$\mathcal{N}\left(\boldsymbol{x}_k;\boldsymbol{m}_{k|k-1}^{(j),i},P_{k|k-1}^{(j),i}\otimes X_k\right)\mathcal{N}\left(\bar{\boldsymbol{z}}_k^{(\boldsymbol{W})};H_k\boldsymbol{x}_k,\frac{B_k^{(j),i}X_k\left(B_k^{(j),i}\right)^{\mathrm{T}}}{|\boldsymbol{W}|}\right)$$
$$=\mathcal{N}\left(\boldsymbol{x}_k;\boldsymbol{m}_{k|k}^{(j,\boldsymbol{W}),i},P_{k|k}^{(j,\boldsymbol{W}),i}\otimes X_k\right)$$
$$\times\mathcal{N}\left(\bar{\boldsymbol{z}}_k^{(\boldsymbol{W})};H_k\boldsymbol{m}_{k|k-1}^{(j),i},\frac{B_k^{(j),i}X_k\left(B_k^{(j),i}\right)^{\mathrm{T}}}{|\boldsymbol{W}|}+H_k(P_{k|k-1}^{(j),i}\otimes X_k)H_k^{\mathrm{T}}\right),\tag{77}$$

$$\mathcal{N}\left(\boldsymbol{x}_k;\boldsymbol{m}_k^{(j,\boldsymbol{W}),i},P_k^{(j,\boldsymbol{W}),i}\otimes X_k\right)\left|s_k^{(j,\boldsymbol{W}),i}\right|^{-\frac{d}{2}}\pi^{-\frac{|\boldsymbol{W}|d}{2}}$$
$$\times|B_k^i|^{-(|\boldsymbol{W}|-1)}|\boldsymbol{W}|^{-\frac{d}{2}}(\delta_k^{p,i})^{\frac{\delta_k^{p,i}d}{2}}\Gamma_d^{-1}\left(\frac{\delta_k^{p,i}}{2}\right)$$
$$\times|Z^{p,i}|^{\frac{\delta_k^{p,i}-d-1}{2}}|V_{k|k-1}^{(j),i}|^{\frac{v_{k|k-1}^{(j),i}-d-1}{2}}\Gamma_d^{-1}\left(\frac{v_{k|k-1}^{(j),i}-d-1}{2}\right)$$
$$\times|X_k|^{-\frac{v_{k|k-1}^{(j),i}+|\boldsymbol{W}|+\delta_k^{p,i}}{2}}2^{-\frac{(v_{k|k-1}^{(j),i}+|\boldsymbol{W}|+\delta_k^{p,i}-d-1)d}{2}}$$
$$\times\operatorname{etr}\left(-\frac{\delta_k^{p,i}(E_k^i)^{-1}Z^{p,i}(E_k^i)^{-\mathrm{T}}+(B_k^i)^{-1}\bar{Z}_k^{(\boldsymbol{W})}(B_k^i)^{-\mathrm{T}}+N_k^{(j,\boldsymbol{W}),i}+V_{k|k-1}^{(j),i}}{2}X_k^{-1}\right).\tag{80}$$

$$2^{-\frac{(|\boldsymbol{W}|-1+\delta_k^{p,i})d}{2}}\pi^{-\frac{(|\boldsymbol{W}|-1)d}{2}}|X_k|^{-\frac{|\boldsymbol{W}|-1+\delta_k^{p,i}}{2}}|B_k^i|^{-(|\boldsymbol{W}|-1)}$$
$$|\boldsymbol{W}|^{-d/2}(\delta_k^{p,i})^{\frac{1}{2}\delta_k^{p,i}d}\Gamma_d^{-1}\left(\frac{\delta_k^{p,i}}{2}\right)|Z^{p,i}|^{\frac{\delta_k^{p,i}-d-1}{2}}$$
$$\operatorname{etr}\left(-\frac{\delta_k^{p,i}(E_k^i)^{-1}Z^{p,i}(E_k^i)^{-T}+(B_k^i)^{-1}\bar{Z}_k^{(\boldsymbol{W})}(B_k^i)^{-\mathrm{T}}}{2}X_k^{-1}\right)$$
$$2^{-\frac{(v_{k|k-1}^{(j),i}-d-1)d}{2}}|V_{k|k-1}^{(j),i}|^{\frac{v_{k|k-1}^{(j),i}-d-1}{2}}\Gamma_d^{-1}\left(\frac{v_{k|k-1}^{(j),i}-d-1}{2}\right)$$
$$|X_k|^{-\frac{v_{k|k-1}^{(j),i}}{2}}\operatorname{etr}\left(-\frac{1}{2}V_{k|k-1}^{(j),i}X_k^{-1}\right).\tag{79}$$

By putting the detailed form PDF of $\mathcal{N}\left(\bar{\boldsymbol{z}}_k^{(\boldsymbol{W})};H_k\boldsymbol{m}_{k|k-1}^{(j),i},s_k^{(j,\boldsymbol{W}),i}X_k^i\right)$ into (79) and simplifying the equation, we can obtain (80), as shown at the top of this page.

With $V_k^{(j,\boldsymbol{W}),i}=V_{k|k-1}^{(j),i}+\delta_k^{p,i}\left(E_k^i\right)^{-1}Z^{p,i}\left(E_k^i\right)^{-\mathrm{T}}+\left(B_k^{(j),i}\right)^{-1}\bar{Z}_k^{(\boldsymbol{W})}\left(B_k^{(j),i}\right)^{-\mathrm{T}}+N_k^{(j,\boldsymbol{W}),i}$ and $v_k^{(j,\boldsymbol{W}),i}=|\boldsymbol{W}|+\delta_k^{p,i}+v_{k|k-1}^{(j),i}$, (80) can be further simplified, i.e.,

$$\mathcal{L}_{k,\mathrm{Ber}}^{(j,\boldsymbol{W}),i}\mathcal{N}\left(\boldsymbol{x};\boldsymbol{m}_k^{(j,\boldsymbol{W}),i},P_k^{(j,\boldsymbol{W}),i}\otimes X\right)$$
$$\times\mathcal{IW}\left(X;v_k^{(j,\boldsymbol{W}),i},V_k^{(j,\boldsymbol{W}),i}\right),\tag{81}$$
$$\mathcal{L}_{k,\mathrm{Ber}}^{(j,\boldsymbol{W}),i}$$
$$=\pi^{-\frac{|\boldsymbol{W}|d}{2}}|Z^{p,i}|^{\frac{\delta_k^{p,i}-d-1}{2}}|s_k^{(j,\boldsymbol{W}),i}|^{-\frac{d}{2}}|\boldsymbol{W}|^{-\frac{d}{2}}|B_k^{(j),i}|^{-(|\boldsymbol{W}|-1)}$$
$$\times(\delta_k^{p,i})^{\frac{\delta_k^{p,i}d}{2}}\Gamma_d^{-1}\left(\frac{\delta_k^{p,i}}{2}\right)|V_k^{(j,\boldsymbol{W}),i}|^{-\frac{v_k^{(j,\boldsymbol{W}),i}-d-1}{2}}$$

TABLE 6. The detailed pseudo code of the proposed JTC-GIW-Ber Filter.

Initialization parameters:

$\boldsymbol{m}_0$, P_0, v_0, V_0, w_0, $\tilde{\mu}_0^i = \frac{1}{n_c}$, $Z^{p,i}$, and $\mathcal{J}_0 = 1$

Input parameters:

$$\left\{\left\{w_{k-1}^{(j),i}, \boldsymbol{m}_{k-1}^{(j),i}, P_{k-1}^{(j),i}, v_{k-1}^{(j),i}, V_{k-1}^{(j),i}, \tilde{\mu}_k^{(j),i}\right\}_{j=1}^{\mathcal{J}_{k-1}}\right\}_{i=1}^{n_c},$$

and the available measurements $\boldsymbol{\mathcal{Z}}_k$ at time k

Step 1: Prediction for birth targets

$q_{k|k-1} = p_{\mathrm{B}}(1-q_{k-1}) + p_{\mathrm{S}} q_{k-1}$
$l = 0$;
for $i = 1, \cdots, n_{\mathrm{B}}$
  for $j = 1, \cdots, \beta_k$
    $l := l + 1$
    $w_{k|k-1}^{(l),i} = \frac{p_{\mathrm{B}}(1-q_{k-1})}{q_{k|k-1}} w_{k,\mathrm{B}}^{(j),i}$, $\tilde{\mu}_{k|k-1}^{(l),i} = \tilde{\mu}_{k,\mathrm{B}}^{(j),i}$
    $\boldsymbol{m}_{k|k-1}^{(l),i} = \boldsymbol{m}_{k,\mathrm{B}}^{(j),i}$, $P_{k|k-1}^{(l),i} = P_{k,\mathrm{B}}^{(j),i}$
    $v_{k|k-1}^{(l),i} = v_{k,B}^{(j),i}$, $V_{k|k-1}^{(l),i} = V_{k,B}^{(j),i}$
  end
end

Step 2: Prediction for existing targets

for $i = 1, \cdots, n_c$
  for $j = 1, \cdots, \mathcal{J}_{k-1}$
    $l := l + 1$
    $w_{k|k-1}^{(l),i} = \frac{p_{\mathrm{S}} q_{k-1}}{q_{k|k-1}} w_{k-1}^{(j),i}$, $\tilde{\mu}_{k|k-1}^{(l),i} = \tilde{\mu}_{k-1}^{(j),i}$
    $\boldsymbol{m}_{k|k-1}^{(l),i} = (F_{k|k-1} \otimes I_d) \boldsymbol{m}_{k-1}^{(j),i}$
    $P_{k|k-1}^{(l),i} = Q_{k|k-1} + F_{k|k-1} P_{k-1}^{(j),i} F_{k|k-1}^{\mathrm{T}}$
    $\lambda_{k-1}^{(j),i} = v_{k-1}^{(j),i} - 2d - 2$
    $v_{k|k-1}^{(l),i} = \frac{2\delta_k \left(\lambda_{k-1}^{(j),i}+1\right)\left(\lambda_{k-1}^{(j),i}-1\right)\left(\lambda_{k-1}^{(j),i}-2\right)}{\left(\lambda_{k-1}^{(j),i}\right)^2 \left(\lambda_{k-1}^{(j),i}+\delta_k\right)} + 2d + 4$
    $V_{k|k-1}^{(l),i} = \frac{\delta_k}{\lambda_{k-1}^{(j),i}} \left(v_{k|k-1,\mathrm{S}}^{(j),i} - 2d - 2\right) A_k V_{k-1}^{(j),i} A_k^{\mathrm{T}}$
  end
end
$\mathcal{J}_{k|k-1} = l$

Step 3: Measurement update for non-detection case

for $i = 1, \cdots, n_c$
  for $j = 1, \cdots, \mathcal{J}_{k|k-1}$
    $w_{k|k}^{(j),i} = (1-p_{\mathrm{D}})^{l_k} w_{k|k-1}^{(j),i}$,
    $\tilde{\mu}_{k|k,\mathrm{ND}}^{(j),i} = \tilde{\mu}_{k|k-1}^{(j),i}$,
    $\boldsymbol{m}_{k|k}^{(j),i} = \boldsymbol{m}_{k|k-1}^{(j),i}$, $P_{k|k}^{(j),i} = P_{k|k-1}^{(j),i}$
    $v_{k|k}^{(j),i} = v_{k|k-1}^{(j),i}$, $V_{k|k}^{(j),i} = V_{k|k-1}^{(j),i}$
  end
end

Step 4: Measurement update for detected case

Compute measurement set $\{\boldsymbol{P}_p\}_{p=1}^{\mathcal{P}}$ and the l_k,
where $\boldsymbol{W} \in \boldsymbol{P}_p$, see[30]
$l = 0, \Delta_k = 0, \Delta_{k,\mathrm{temp}} = 0$
for $p = 1, \cdots, \mathcal{P}$
  for $\omega = 1, \cdots, |P_p|$
    $l := l + 1$
    $\psi_k^{(\boldsymbol{W}_p^\omega)} = \frac{l_k!}{(l_k - |\boldsymbol{W}_p^\omega|)!} \frac{p_{\mathrm{D}}^{|\boldsymbol{W}_p^\omega|}}{(1-p_{\mathrm{D}})^{|\boldsymbol{W}_p^\omega| - l_k}}$
    $\bar{\boldsymbol{z}}_k^{(\boldsymbol{W}_p^\omega)} = \frac{1}{|\boldsymbol{W}_p^\omega|} \sum_{\boldsymbol{z}_k \in \boldsymbol{W}_p^\omega} \boldsymbol{z}_k$

TABLE 6. *(Continued.)* The detailed pseudo code of the proposed JTC-GIW-Ber Filter.

$$\bar{\boldsymbol{Z}}_k^{(\boldsymbol{W}_p^\omega)} = \sum_{\boldsymbol{z}_k \in \boldsymbol{W}_p^\omega} \left(\boldsymbol{z}_k - \bar{\boldsymbol{z}}_k^{(\boldsymbol{W}_p^\omega)}\right)\left(\boldsymbol{z}_k - \bar{\boldsymbol{z}}_k^{(\boldsymbol{W}_p^\omega)}\right)^{\mathrm{T}}$$

for $i = 1, \cdots, n_c$
  for $j = 1, \cdots, \mathcal{J}_{k|k-1}$

$$s_k^{(j,\boldsymbol{W}_p^\omega),i} = \frac{|B_k^{(j),i}|^{2/d}}{|\boldsymbol{W}_p^\omega|} + \boldsymbol{h}_k P_{k|k-1}^{(j),i} \boldsymbol{h}_k^{\mathrm{T}}$$

$$\boldsymbol{k}_k^{(j,\boldsymbol{W}_p^\omega),i} = P_{k|k-1}^{(j,\boldsymbol{W}_p^\omega),i} \boldsymbol{h}_k^{\mathrm{T}} \left(s_k^{(j,\boldsymbol{W}_p^\omega),i}\right)^{-1}$$

$$N_k^{(j,\boldsymbol{W}_p^\omega),i} = \left(s_k^{(j,\boldsymbol{W}_p^\omega),i}\right)^{-1} \left(\bar{\boldsymbol{z}}_k^{(\boldsymbol{W}_p^\omega)} - H_k \boldsymbol{m}_{k|k-1}^{(j),i}\right) \left(\bar{\boldsymbol{z}}_k^{(\boldsymbol{W}_p^\omega)} - H_k \boldsymbol{m}_{k|k-1}^{(j),i}\right)^{\mathrm{T}}$$

$$\boldsymbol{m}_k^{(j+\mathcal{J}_{k|k-1}l),i} = \boldsymbol{m}_{k|k-1}^{(j),i} + \left(\boldsymbol{k}_k^{(j,\boldsymbol{W}_p^\omega),i} \otimes I_d\right)\left(\bar{\boldsymbol{z}}_k^{(\boldsymbol{W}_p^\omega)} - H_k \boldsymbol{m}_{k|k-1}^{(j),i}\right)$$

$$P_k^{(j+\mathcal{J}_{k|k-1}l),i} = P_{k|k-1}^{(j),i} - \boldsymbol{k}_k^{(j,\boldsymbol{W}_p^\omega),i} s_k^{(j,\boldsymbol{W}_p^\omega),i} \left(\boldsymbol{k}_k^{(j,\boldsymbol{W}_p^\omega),i}\right)^{\mathrm{T}}$$

$$v_k^{(j+\mathcal{J}_{k|k-1}l),i} = |\boldsymbol{W}_p^\omega| + \delta_k^{p,i} + v_{k|k-1}^{(j),i}$$

$$V_k^{(j+\mathcal{J}_{k|k-1}l),i} = V_{k|k-1}^{(j),i} + \delta_k^{p,i} (E_k^i)^{-1} Z^{p,i} (E_k^i)^{-\mathrm{T}} + \left(B_k^{(j),i}\right)^{-1} \bar{Z}_k^{(\boldsymbol{W}_p^\omega)} \left(B_k^{(j),i}\right)^{-\mathrm{T}} + N_k^{(j,\boldsymbol{W}_p^\omega),i}$$

$$\mathcal{L}_{k,\mathrm{Ber}}^{(j,\boldsymbol{W}_p^\omega),i} = \tilde{\Lambda}_k^{(j+\mathcal{J}_{k|k-1}l),i} = \pi^{-\frac{|\boldsymbol{W}_p^\omega| d}{2}} |Z^{p,i}|^{\frac{\delta_k^{p,i}-d-1}{2}} \left|s_k^{(j,\boldsymbol{W}_p^\omega),i}\right|^{-\frac{d}{2}} |\boldsymbol{W}_p^\omega|^{-\frac{d}{2}} \left|B_k^{(j),i}\right|^{-\frac{|\boldsymbol{W}_p^\omega|-1}{2}} (\delta_k^{p,i})^{\frac{\delta_k^{p,i} d}{2}} \Gamma_d^{-1}\left(\frac{\delta_k^{p,i}}{2}\right) \Gamma_d\left(\frac{v_k^{(j,\boldsymbol{W}_p^\omega),i}-d-1}{2}\right) \left|V_{k|k-1}^{(j),i}\right|^{\frac{v_{k|k-1}^{(j),i}-d-1}{2}} \left|V_k^{(j,\boldsymbol{W}_p^\omega),i}\right|^{-\frac{v_k^{(j,\boldsymbol{W}_p^\omega),i}-d-1}{2}} \Gamma_d^{-1}\left(\frac{v_{k|k-1}^{(j),i}-d-1}{2}\right)$$

$$\tilde{\nabla}_k = \sum_{i=1}^{n_c} \tilde{\Lambda}_k^{(j+\mathcal{J}_{k|k-1}l),i} \tilde{\mu}_{k|k-1}^{(j),i},$$

$$\tilde{\mu}_k^{(j+\mathcal{J}_{k|k-1}l),i} = \left(\tilde{\nabla}_k\right)^{-1} \tilde{\Lambda}_k^{(j+\mathcal{J}_{k|k-1}l),i} \tilde{\mu}_{k|k-1}^{(j),i}$$

$$w_k^{(j+\mathcal{J}_{k|k-1}l),i} = \psi_k^{(\boldsymbol{W}_p^\omega)} \beta_{\mathrm{FA},k}^{-|\boldsymbol{W}_p^\omega|} \mathcal{L}_{k,\mathrm{Ber}}^{(j,\boldsymbol{W}_p^\omega),i} w_{k|k-1}^{(j),i}$$

  end
 end
end

$$\Delta_{k,\mathrm{temp}} = \Delta_{k,\mathrm{temp}} + \sum_{i=1}^{n_c} \sum_{j=1}^{\mathcal{J}_{k|k-1}} w_k^{(j+\mathcal{J}_{k|k-1}l),i}$$

end
$\mathcal{J}_k = \mathcal{J}_{k|k-1} + l\mathcal{J}_{k|k-1}$
$\Delta_k = 1 - (1-p_d)^{l_k}$
$w_k = \frac{w_k}{1-\Delta_k}$

Output parameters:

$$\left\{\left\{w_k^{(j),i}, \boldsymbol{m}_k^{(j),i}, P_k^{(j),i}, v_k^{(j),i}, V_k^{(j),i}, \tilde{\mu}_k^{(j),i}\right\}_{j=1}^{\mathcal{J}_k}\right\}_{i=1}^{n_c}.$$

State extraction:

$j^* = \underset{j}{\operatorname{argmax}}\, w_k^{(j),i}$, $\hat{\boldsymbol{m}}_k^i = \boldsymbol{m}_k^{(j^*),i}$, $\hat{P}_k^i = P_k^{(j^*),i}$,
$\hat{v}_k^i = v_k^{(j^*),i}$, $\hat{V}_k^i = V_k^{(j^*),i}$, and $\hat{\mu}_k^i = \tilde{\mu}_k^{(j^*),i}$.

$$\boldsymbol{m}_k = \sum_{i=1}^{n_c} \hat{\mu}_k^i \hat{\boldsymbol{m}}_k^i, \; P_k = \sum_{i=1}^{n_c} \hat{\mu}_k^i \hat{P}_k^i,$$

$$v_k = \sum_{i=1}^{n_c} \hat{\mu}_k^i \hat{v}_k^i, \; V_k = \sum_{i=1}^{n_c} \hat{\mu}_k^i \hat{V}_k^i.$$

Output estimated state:

Kinematic state: $\hat{\boldsymbol{x}}_k = \boldsymbol{m}_k$
Extent state: $\hat{X}_k = V_k/(v_k - 2d - 2)$

$$\times \Gamma_d^{-1}\left(\frac{v_{k|k-1}^{(j),i}-d-1}{2}\right)\Gamma_d\left(\frac{v_k^{(j,\boldsymbol{W}),i}-d-1}{2}\right)$$
$$\times |V_{k|k-1}^{(j),i}|^{\frac{v_{k|k-1}^{(j),i}-d-1}{2}}. \quad (82)$$

For target classification, the calculation $\tilde{\Lambda}_k^{(j,\boldsymbol{W}),i}$ is key to obtain the updated class probabilities according to (30). Therefore, based on (29), we can get

$$\begin{aligned}
&\tilde{\Lambda}_k^{(j,\boldsymbol{W})i}\\
&=\int p(\boldsymbol{\mathcal{Z}_k}|\boldsymbol{x}_k,X_k,c^i,\boldsymbol{\mathcal{Z}}^{k-1})p(\boldsymbol{x}_k,X_k|c^i,\boldsymbol{\mathcal{Z}}^{k-1})d\boldsymbol{x}_k dX_k\\
&=\int (2\pi)^{-\frac{(|\boldsymbol{W}|-1)d}{2}}|B_k^i X_k (B_k^i)^{\mathrm{T}}|^{-\frac{|\boldsymbol{W}|-1}{2}}|\boldsymbol{W}|^{-\frac{d}{2}}\\
&\quad\times \mathrm{etr}\left\{-\frac{\bar{Z}_k^{(\boldsymbol{W})}}{2}\left(B_k^i X_k^i (B_k^i)^{\mathrm{T}}\right)^{-1}\right\}\\
&\quad\times\mathcal{N}\left(\bar{\boldsymbol{z}}_k^{(\boldsymbol{W})};H_k\boldsymbol{x}_k,\frac{B_k^i X_k (B_k^i)^{\mathrm{T}}}{|\boldsymbol{W}|}\right)\\
&\quad\times\mathcal{W}\left(Z^{p,i};\delta_k^{p,i},E_k^i X_k (E_k^i)^{\mathrm{T}}/\delta_k^{p,i}\right)\\
&\quad\times\mathcal{N}\left(\boldsymbol{x}_k;\boldsymbol{m}_{k|k-1}^{(j),i},P_{k|k-1}^{(j),i}\otimes X_k\right)\\
&\quad\times\mathcal{IW}\left(X_k;v_{k|k-1}^{(j),i},V_{k|k-1}^{(j),i}\right)d\boldsymbol{x}_k dX_k\\
&=\int\mathcal{N}\left(\boldsymbol{x}_k;\boldsymbol{m}_k^{(j,\boldsymbol{W}),i},P_k^{(j,\boldsymbol{W}),i}\otimes X_k\right)\\
&\quad\times\mathcal{IW}\left(X_k;v_k^{(j,\boldsymbol{W}),i},V_k^{(j,\boldsymbol{W}),i}\right)\\
&\quad\times\pi^{-\frac{|\boldsymbol{W}|d}{2}}|Z^{p,i}|^{\frac{\delta_k^{p,i}-d-1}{2}}|s_k^{(j,\boldsymbol{W}),i}|^{-\frac{d}{2}}|\boldsymbol{W}|^{-\frac{d}{2}}|B_k^i|^{-(|\boldsymbol{W}|-1)}\\
&\quad\times(\delta_k^{p,i})^{\frac{\delta_k^{p,i}d}{2}}\Gamma_d^{-1}\left(\frac{\delta_k^{p,i}}{2}\right)|V_k^{(j,\boldsymbol{W}),i}|^{-\frac{v_k^{(j,\boldsymbol{W}),i}-d-1}{2}}\Gamma_d\\
&\quad\times\left(\frac{v_k^{(j,\boldsymbol{W}),i}-d-1}{2}\right)\\
&\quad\times|V_{k|k-1}^{(j),i}|^{\frac{v_{k|k-1}^{(j),i}-d-1}{2}}\Gamma_d^{-1}\left(\frac{v_{k|k-1}^{(j),i}-d-1}{2}\right)d\boldsymbol{x}_k dX_k\\
&=\pi^{-\frac{|\boldsymbol{W}|d}{2}}|Z^{p,i}|^{\frac{\delta_k^{p,i}-d-1}{2}}|s_k^{(j,\boldsymbol{W}),i}|^{-\frac{d}{2}}|\boldsymbol{W}|^{-\frac{d}{2}}\\
&\quad\times|B_k^i|^{-(|\boldsymbol{W}|-1)}(\delta_k^{p,i})^{\frac{\delta_k^{p,i}d}{2}}\Gamma_d^{-1}\left(\frac{\delta_k^{p,i}}{2}\right)|V_k^{(j,\boldsymbol{W}),i}|^{-\frac{v_k^{(j,\boldsymbol{W}),i}-d-1}{2}}\\
&\quad\times\Gamma_d\left(\frac{v_k^{(j,\boldsymbol{W}),i}-d-1}{2}\right)|V_{k|k-1}^{(j),i}|^{\frac{v_{k|k-1}^{(j),i}-d-1}{2}}\Gamma_d^{-1}\\
&\quad\times\left(\frac{v_{k|k-1}^{(j),i}-d-1}{2}\right). \quad (83)
\end{aligned}$$

All the parameters of JTC-GIW-Ber filter are obtained.

APPENDIX B
THE DETAILED PSEUDO CODE OF JTC-GIW-BER FILTER

See Table 6.

REFERENCES

[1] J. Lan and X. R. Li, "Joint tracking and classification of extended object using random matrix," in *Proc. 16th Int. Conf. Inf. Fusion*, Istanbul, Turkey, Jul. 2013, pp. 1550–1557.
[2] W. Cao, J. Lan, and X. R. Li, "Joint tracking and classification based on recursive joint decision and estimation using multi-sensor data," in *Proc. 17th Int. Conf. Inf. Fusion*, Salamanca, Spain, Jul. 2014, pp. 1–8.
[3] W. Cao, J. Lan, and X. R. Li, "Extended object tracking and classification using radar and ESM sensor data," *IEEE Signal Process. Lett.*, vol. 25, no. 1, pp. 90–94, Jan. 2018.
[4] B. Ristic, N. Gordon, and A. Bessell, "On target classification using kinematic data," *Inf. Fusion*, vol. 5, no. 1, pp. 15–21, Mar. 2004.
[5] D. Angelova and L. Mihaylova, "Joint target tracking and classification with particle filtering and mixture Kalman filtering using kinematic radar information," *Digit. Signal Process.*, vol. 16, no. 2, pp. 180–204, Mar. 2006.
[6] S. Challa and G. W. Pulford, "Joint target tracking and classification using radar and ESM sensors," *IEEE Trans. Aerosp. Electron. Syst.*, vol. 37, no. 3, pp. 1039–1055, Jul. 2001.
[7] H. Jiang, K. Zhan, and L. Xu, "Joint tracking and classification with constraints and reassignment by radar and ESM," *Digit. Signal Process.*, vol. 40, pp. 213–223, May 2015.
[8] K. Granström, M. Baum, and S. Reuter, "Extended object tracking: Introduction, overview, and applications," *J. Adv. Inf. Fusion*, vol. 12, no. 2, pp. 139–174, Dec. 2017.
[9] J. W. Koch, "Bayesian approach to extended object and cluster tracking using random matrices," *IEEE Trans. Aerosp. Electron. Syst.*, vol. 44, no. 3, pp. 1042–1059, Jul. 2008.
[10] M. Feldmann, D. Fränken, and W. Koch, "Tracking of extended objects and group targets using random matrices," *IEEE Trans. Signal Process.*, vol. 59, no. 4, pp. 1409–1420, Apr. 2011.
[11] J. Lan and X. R. Li, "Tracking of extended object or target group using random matrix: New model and approach," *IEEE Trans. Aerosp. Electron. Syst.*, vol. 52, no. 6, pp. 2973–2989, Dec. 2016.
[12] M. Baum and U. D. Hanebeck, "Shape tracking of extended objects and group targets with star-convex RHMs," in *Proc. 14th Int. Conf. Inf. Fusion*, Chicago, IL, USA, Jul. 2011 pp. 1–8.
[13] M. Baum and U. D. Hanebeck, "Extended object tracking with random hypersurface models," *IEEE Trans. Aerosp. Electron. Syst.*, vol. 50, no. 1, pp. 149–159, Jan. 2014.
[14] M. Baum, B. Noack, and U. D. Hanebeck, "Extended object and group tracking with elliptic random hypersurface models," in *Proc. 13th Int. Conf. Inf. Fusion*, Edinburgh, U.K., Jul. 2010, pp. 1–8.
[15] N. Wahlström and E. Özkan, "Extended target tracking using Gaussian processes," *IEEE Trans. Signal Process.*, vol. 63, no. 16, pp. 4165–4178, Aug. 2015.
[16] T. Hirscher, A. Scheel, S. Reuter, and K. Dietmayer, "Multiple extended object tracking using Gaussian processes," in *Proc. 19th Int. Conf. Inf. Fusion*, Heidelberg, Germany, Jul. 2016, pp. 868–875.
[17] L. Sun, J. Lan, and X. R. Li, "Joint tracking and classification of extended object based on support functions," *IET Radar Sonar Navigat.*, vol. 12, no. 7, pp. 685–693, Jul. 2018.
[18] C. Magnant, S. Kemkemian, and L. Zimmer, "Joint tracking and classification for extended targets in maritime surveillance," in *Proc. IEEE Radar Conf.*, Oklahoma City, OK, USA, Apr. 2018, pp. 1117–1122.
[19] Q. Hu, H. Ji, and Y. Zhang, "A standard PHD filter for joint tracking and classification of maneuvering extended targets using random matrix," *Signal Process.*, vol. 144, pp. 352–363, Mar. 2018.
[20] R. P. S. Mahler, "Multitarget Bayes filtering via first-order multitarget moments," *IEEE Trans. Aerosp. Electron. Syst.*, vol. 39, no. 4, pp. 1152–1178, Oct. 2003.
[21] B.-N. Vo, S. Singh, and A. Doucet, "Sequential Monte Carlo methods for multitarget filtering with random finite sets," *IEEE Trans. Aerosp. Electron. Syst.*, vol. 41, no. 4, pp. 1224–1245, Oct. 2005.
[22] B. Ristic, B.-T. Vo, B.-N. Vo, and A. Farina, "A tutorial on Bernoulli filters: Theory, implementation and applications," *IEEE Trans. Signal Process.*, vol. 61, no. 13, pp. 3406–3430, Jul. 2013.
[23] W. Yang, Z. Wang, Y. Fu, X. Pan, and X. Li, "Joint detection, tracking and classification of a manoeuvring target in the finite set statistics framework," *IET Signal Process.*, vol. 9, no. 1, pp. 10–20, Feb. 2015.
[24] L. Legrand, A. Giremus, E. Grivel, L. Ratton, and B. Joseph, "Bernoulli filter based algorithm for joint target tracking and classification in a cluttered environment," in *Proc. IEEE Int. Conf. Acoust., Speech Signal Process.*, New Orleans, LA, USA, Mar. 2017, pp. 4396–4400.

[25] G. Vivone, P. Braca, K. Granström, A. Natale, and J. Chanussot, "Converted measurements Bayesian extended target tracking applied to X-band marine radar data," *J. Adv. Inf. Fusion*, vol. 12, no. 2, pp. 189–210, Dec. 2017.
[26] G. Vivone, P. Braca, K. Granstrom, and P. Willett, "Multistatic Bayesian extended target tracking," *IEEE Trans. Aerosp. Electron. Syst.*, vol. 52, no. 6, pp. 2626–2643, Dec. 2016.
[27] K. Granström, A. Natale, P. Braca, G. Ludeno, and F. Serafino, "Gamma Gaussian inverse Wishart probability hypothesis density for extended target tracking using X-band marine radar data," *IEEE Trans. Geosci. Remote Sens.*, vol. 53, no. 12, pp. 6617–6631, Dec. 2015.
[28] R. P. S. Mahler, *Statistical Multisource-Multitarget Information Fusion*. Norwood, MA, USA: Artech House, 2007.
[29] R. P. S. Mahler, *Advances in Statistical Multisource-Multitarget Information Fusion*. Norwood, MA, USA: Artech House, 2014.
[30] A. Eryildirim and M. B. Guldogan, "A Bernoulli filter for extended target tracking using random matrices in a UWB sensor network," *IEEE Sensors J.*, vol. 16, no. 11, pp. 4362–4373, Jun. 2016.
[31] D. Schuhmacher, B.-T. Vo, and B.-N. Vo, "A consistent metric for performance evaluation of multi-object filters," *IEEE Trans. Signal Process.*, vol. 56, no. 8, pp. 3447–3457, Aug. 2008.
[32] B. Li, C. Mu, Y. Bai, J. Bi, and L. Wang, "Ellipse fitting based approach for extended object tracking," *Math. Problems Eng.*, vol. 2014, May 2014, Art. no. 632815.
[33] B. N. Vo and W. K. Ma, "The Gaussian mixture probability hypothesis density filter," *IEEE Trans. Signal Process.*, vol. 54, no. 11, pp. 4091–4104, Nov. 2006.

LIPING WANG received the B.E. and M.E. degrees in communication engineering and signal and information processing from Shandong University, Weihai, China, in 2014 and 2017, respectively. She is currently pursuing the Ph.D. degree in signal and information processing with the National University of Defense Technology (NUDT), Changsha, China. Her current research interests include extended target tracking and target joint tracking and classification.

YUAN HUANG received the B.E. and M.E. degrees in information engineering and information and communication engineering from the National University of Defense Technology (NUDT), Changsha, China, in 2013 and 2015, respectively, where he is currently pursuing the Ph.D. degree. His research interests include extended target tracking and joint tracking and classification.

RONGHUI ZHAN was born in Jiangxi, China, in 1978. He received the M.S. and Ph.D. degrees in information and communication engineering from the National University of Defense Technology (NUDT), Changsha, China, in 2003 and 2007, respectively.

He is currently an Associate Professor with the ATR Laboratory, NUDT. His current research interests include radar signal processing, automatic target recognition, and the Bayesian estimation theory with an emphasis on target tracking.

JUN ZHANG was born in Hunan, China, in 1973. He received the M.S. and Ph.D. degrees from the National University of Defense Technology (NUDT), Changsha, China, in 1998 and 2002, respectively.

He is currently a Professor with the ATR Laboratory, NUDT. His current research interests include radar signal processing, radar systems, and automation target recognition.